

# Rapid and Uniform Cell Seeding on Fibrin Microthreads to Generate Tissue Engineered Microvessels



A thesis submitted to the faculty of Worcester Polytechnic Institute in partial fulfillment of the requirements for the Degree of Master of Science

May 2010

Submitted by

Darshan Pravin Parekh

Department of Biomedical Engineering

---

Approved by:

---

Glenn Gaudette, PhD  
Assistant Professor

Department of Biomedical Engineering

Committee member

---

George Pins, PhD  
Associate Professor

Department of Biomedical Engineering

Committee member

---

Marsha Rolle, PhD

Assistant Professor

Department of Biomedical Engineering

Thesis advisor

## **Acknowledgements**

I would like to express gratitude to my research advisor Dr. Marsha Rolle for her constant guidance and innovative ideas that made this project a knowledgeable and exciting journey. To add, my heartfelt thanks to my committee members Dr. Glenn Gaudette and Dr. George Pins for their support throughout and directing me with their valuable feedback.

All the help from Sharon Shaw for histology, Victoria Huntress for her endless help in confocal microscopy and Neil Whitehouse for machining that took this project to the next level is highly appreciated. A special thanks to Tracy Gwyther for being an ideal mentor. Her contributions in teaching the basic lab skills and directing at critical points of this project are invaluable. I would also like to thank Shawn Carey for providing the fibrin microthreads and Jeremy Skorinko for helping with CAD drawings. Not to forget the Rolle lab members and my friends Stephanie Kaszuba, Amanda Zoë Reidinger, Jason Hu and Carlos Donado who made this project an enjoyable experience.

Heartfelt thanks to my beloved Kshama Doshi for standing by me throughout in the rough and joyful times of this thesis. Last but not the least; I would like to make a special mention of my family members: father Pravin G Parekh, mother Purnima P Parekh, brother Bhavin P Parekh and sister-in-law Rachana B Parekh for giving me the mental strength and support to perform at my best.

## **Abstract**

A wide variety of techniques have been explored to synthesize small diameter tissue engineered blood vessels. Toward this end, we are exploring direct cell seeding and culture on tubular mandrels to create engineered vascular tissues. In the present study, v-shaped channels cast from polydimethyl siloxane (PDMS) were used as cell seeding wells. Fibrin microthreads placed in the chamber were used as model tubular seeding mandrels. Human mesenchymal stem cells (hMSCs) were seeded onto fibrin microthreads in v-shaped channels for 4 hours. Cell attachment to the microthreads was confirmed visually by Hoechst nuclear staining and a cell quantification assay showed that  $5,114 \pm 339$  cells attached per 1 cm fibrin microthread sample ( $n = 6$ ). Fibrin microthreads were completely degraded by hMSCs within 5 days of culture, therefore UV crosslinking was used to increase their mechanical strength and prolong the amount of time cells could be cultured on fibrin microthreads and generate tubular tissue constructs. Cell attachment was unaffected on UV-crosslinked microthreads compared to uncrosslinked microthreads, resulting in a count of  $4,944 \pm 210$  cells per 1 cm of fibrin microthread sample ( $n = 3$ ). Long term culture of the hMSCs on the UV-crosslinked fibrin microthreads showed an increase in cell number over time to  $11,198 \pm 582$  cells per cm of microthread after 7 days with 92% cell viability (CYQUANT NF/DEAD staining) and evidence of cell proliferation. The results show that the v-well cell seeding technique was effective in promoting rapid hMSC attachment on UV-crosslinked fibrin microthreads and encouraged their growth, maintained viability and also promoted their proliferation over the culture period. In conclusion, the technique could serve as an efficient model system for rapid formation of tissue engineered vascular grafts.

## Table of Contents

Chapter 1: Introduction .....	9
Chapter 2: Background .....	13
2.1 Physiology and anatomy of a blood vessel .....	13
2.2 Clinical significance.....	14
2.3 Blood vessel replacements .....	15
2.3.1 Synthetic blood vessel substitutes.....	15
2.3.2 Tissue engineered blood vessels .....	16
2.3.3 Fully biologic tissue engineered blood vessels .....	18
2.4 Importance of cell seeding technique.....	19
2.4.1 Hanging drop seeding technique.....	20
2.4.2 V-shaped cell seeding chamber.....	20
2.5 Bone marrow derived human mesenchymal stem cells .....	21
2.6 Fibrin microthreads as tubular seeding mandrel .....	23
Chapter 3: Materials and Methods .....	24
3.1 Bone marrow-derived human mesenchymal stem cell (hMSC) culture .....	24
3.2 Production of fibrin microthreads .....	25
3.3 Cell seeding techniques.....	26
3.3.1 Hanging drop cell seeding technique .....	26
3.3.2 V-shaped cell seeding channels .....	28
3.4 UV crosslinking of fibrin microthreads .....	31
3.5 Characterization of cell attachment and distribution .....	31
3.5.1 Hoechst staining.....	31
3.5.2 Phalloidin staining.....	32
3.6 Cell quantification - CyQuant NF .....	32



3.7 Cytotoxicity assay .....	34
3.8 Click-it EdU cell proliferation assay.....	36
3.9 Statistical analysis.....	37
3.10 Confocal imaging technique .....	38
3.11 Assessment of hMSC growth on fibrin microthreads in culture.....	38
Chapter 4: Results.....	40
4.1 Comparison of hanging drop seeding and v-well seeding .....	40
4.1.1 Characterization of cell attachment and distribution by Hoechst imaging for hanging drop seeding .....	40
4.1.2 Characterization of cell attachment and distribution by Hoechst and phalloidin imaging by v-well seeding .....	42
4.1.3 Comparing cell attachment using CyQuant NF assay for the two seeding methods .....	44
4.1.4 Assessing cell viability with the CYQUANT NF/DEAD assay for v-well seeding .....	46
4.2 Long term culture of hMSC seeded fibrin microthreads .....	47
4.2.1 Characterization of cell attachment and distribution by Hoechst and phalloidin imaging .....	47
4.2.2 Quantification of cell attachment using CyQuant NF assay .....	48
4.2.3 Assessing cell viability using live dead assay.....	48
4.2.4 Quantification of proliferating cells using Click-it EdU assay .....	49
4.3 hMSC seeding on UV-crosslinked fibrin microthreads in v-shaped chambers .....	50
4.3.1 Characterization of cell attachment and distribution by Hoechst and phalloidin imaging .....	50
4.3.2 Quantification of cell attachment using CyQuant NF assay .....	51
4.3.3 Assessing cell viability via CyQuant NF/DEAD assay .....	51
4.4 Long term culture of hMSCs on UV crosslinked fibrin microthreads.....	52
4.4.1 Characterization of cell attachment and distribution by Hoechst and phalloidin imaging .....	52
4.4.2 Quantification of cell number as a function of culture time using CyQuant NF assay.....	55
4.4.3 Assessing cell viability by CYQUANT NF/DEAD assay .....	56

4.4.4 Quantification of proliferating cells using Click-it EdU assay .....	58
Chapter 5: Discussion .....	60
5.1 Hanging drop seeding compared to seeding in v-shaped chambers.....	60
5.2 Long term culture in v-shaped chambers.....	63
5.2.1 Advantages of UV crosslinked fibrin microthread .....	63
5.2.2 Cell attachment characterization.....	64
Conclusions.....	68
Chapter 6: Future work .....	69
6.1 Monolayer cell attachment post-seeding.....	69
6.2 hMSC characterization.....	70
6.3 Longer hMSC culture on fibrin microthreads in v-wells.....	71

## Table of Figures

Figure 1. Schematic showing components of the direct cell seeding technique .....	11
Figure 2. Schematic of a hanging drop seeding technique [32] .....	20
Figure 3. Schematic of a v-shaped cell seeding chamber .....	21
Figure 4. Human mesenchymal stem cells in culture (passage 8) .....	24
Figure 5. Schematic of the extrusion of fibrin microthreads and scanning electron micrograph of the fibrin microthreads [53] .....	25
Figure 6. Schematic of the hanging drop seeding method .....	26
Figure 7. Image of a fibrin microthread glued onto a PDMS ring .....	27
Figure 8. Schematic showing the preparation and dimensions of the v-shaped PDMS chambers .....	29
Figure 9. Schematic of hMSC seeding onto fibrin microthreads in v-shaped PDMS chambers .....	30
Figure 10. Schematic of cell harvesting from fibrin microthreads and quantification of cell number using the CyQuant NF protocol .....	33
Figure 11. Graph of the standard curve for CyQuant NF .....	34
Figure 12. Schematic of Click-It EdU cell proliferation assay .....	36
Figure 13. Assessment of cell attachment by hanging drop seeding by Hoechst dye .....	41
Figure 14. Regions of an hMSC-seeded fibrin microthread after 4 hours of hanging drop seeding .....	41
Figure 15. Assessment of hMSC attachment in v-shaped chambers by Hoechst and Phalloidin .....	43
Figure 16. CyQuant NF quantification of hMSC attachment by hanging drop and v-well seeding .....	45
Figure 17. Stained dead cells and phase contrast image of a fibrin microthread seeded with hMSCs for 4h .....	47
Figure 18. Hoechst - phalloidin stained microthread and phase contrast image after 3 days cultured in v-well chambers .....	48
Figure 19. DEAD staining of hMSCs and phase contrast image of microthreads in v-shaped chambers after 3 days .....	49
Figure 20. Analysis of hMSC proliferation by Click-it EdU staining and phase contrast .....	49
Figure 21. Assessment of cell attachment on UV crosslinked fibrin microthreads .....	51

Figure 22. DEAD cells on UV cross-linked fibrin microthreads and phase contrast .....	52
Figure 23. Hochst-Phalloidin merged and phase contrast images of UV cross-linked fibrin microthreads cultured with hMSCs for 3 days, 5 days and 7 days .....	53
Figure 24. Graph showing comparison of cell layer thickness .....	54
Figure 25. Quantification of cells on UV crosslinked fibrin microthreads after 4 hours of seeding on fibrin microthreads followed by culture for 3, 5 or 7 days .....	55
Figure 26. DEAD cells on UV crosslinked fibrin microthreads and phase contrast images .....	57
Figure 27. Percentage of dead cells on UV crosslinked fibrin microthreads after 4 hours of seeding .....	58
Figure 28. EdU-Hoechst stained images of UV crosslinked fibrin microthreads seeded with hMSCs .....	59
Figure 29. Schematic of possible errors by hanging drop seeding.....	62

## Chapter 1: Introduction

Coronary artery disease (CAD) is the most common form of cardiovascular diseases affecting approximately 17.6 million Americans with the expenditure on treatment and research amounting to \$177 billion annually [1]. The major causative factor for CAD is atherosclerosis, an inflammatory disease that causes blockage of the artery and hence results in reduced blood flow.

Percutaneous coronary intervention (PCI) and coronary artery bypass graft (CABG) surgery are the two widely used treatments for CAD, with the optimal of the two still being a topic of debate [2-4]. CABG still remains a better option in terms of being more durable for diabetics, older patients and the in case of severe extent of disease [2-6]. For CABG surgery, autologous vessels are the first choice of sources for vascular grafts. However, availability of autologous replacement grafts is limited due to the patient's health condition or due to previously performed multiple surgeries. Use of synthetic grafts is limited to the application of large diameter (> 6mm) blood vessels only [7-11]. The approach of tissue engineering of blood vessels has therefore gained much importance in recent years. Using decellularized grafts, seeding cells in biopolymer gels and on biodegradable scaffolds are widely studied techniques for developing tissue engineered blood vessels (TEBV) [12]. However, these techniques still face the problems of weak mechanical properties, degradation, foreign body response, and thrombus formation [13,14].

L'Heureux et al demonstrated a novel technique for developing fully biologic TEBV by rolling cell sheets around a tubular mandrel [15]. The major hindrance for the practical application of this technique is the time required to produce the final graft and the tissue

manipulations involved in wrapping the graft and removing the mandrel. However, this approach demonstrates that the cells are capable of self-assembling, forming their own matrix and remodeling into a new tissue. Hence, the concept of developing fully biologic blood vessels combined with a simple, scaffold-free technique that would enable fast and simple construct formation could prove to be a more practical and efficient approach. One such approach involves seeding cells directly onto tubular mandrels wherein the cells attach and grow to form a tubular cell construct. Ideally, a tubular mandrel made from a biodegradable material may be beneficial in that it would eliminate the step of mandrel removal.

The approach of direct cell seeding on tubular mandrels has been studied previously. Neumann et al [16] seeded rat aortic smooth muscle cells onto laminin-coated nylon strands for 21-28 days before subjecting them to perfusion bioreactor system. In another approach, magnetically labeled cells were seeded directly onto a tubular shaped collagen membrane which was subjected to magnetic forces [17]. These direct cell seeding techniques were effective in developing tubular constructs from cells only, however it still required either mandrel removal for releasing the tubular cell construct or application of external forces to enhance cell attachment. Although these approaches are promising, there is room for improvement in designing a simple, direct cell seeding technique that would overcome the shortcomings of the seeding techniques studied until now.

**This thesis project focused on developing a direct cell seeding technique that would allow cells to attach rapidly, distribute evenly around a tubular mandrel and form a tubular tissue without any external forces or tissue/mandrel manipulations.**

In order to develop a direct cell seeding approach for blood vessel generation, we focused on three basic components: 1) a tubular mandrel of suitable material for cells to adhere which would degrade over time leaving a lumen, 2) cells to be seeded and 3) lastly, an effective method to deliver these cells onto the mandrel (Figure 1).

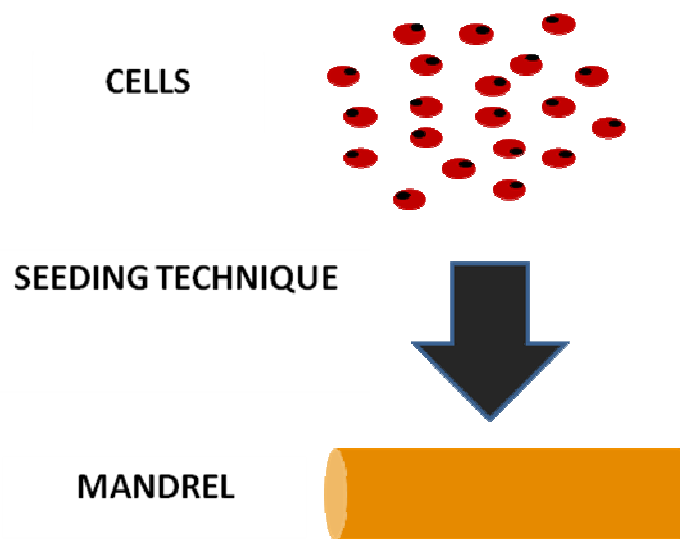


**Figure 1. Schematic showing components of the direct cell seeding technique**

In order to meet these requirements, we developed a novel cell seeding technique, referred to as ‘v-shaped cell seeding technique’ hereafter. Biodegradable fibrin microthreads were used as model tubular seeding mandrels and human mesenchymal stem cells (hMSCs) were seeded onto these fibrin microthreads in the v-wells. For comparison, hMSCs were seeded on

fibrin microthreads using ‘hanging drop seeding’, the current seeding technique used in our lab. A detailed explanation of the concept and rationale for pursuing these particular materials and approaches will follow in the background section.

**Development and validation of the novel seeding technique was accomplished through the following Specific Aims:**

**Specific Aim 1: To develop a consistent, reproducible cell seeding technique to allow rapid cell attachment along a tubular seeding mandrel.**

In order to assess hMSC attachment on fibrin microthreads, cells were quantified using CyQuant NF assay after 4 hours of v-well seeding and were analyzed by Hoechst staining for cell distribution. The results were compared to those using the hanging drop technique to determine which method resulted in a better seeding efficiency. In order to compare consistency and reproducibility of the two seeding techniques, variability of cell attachment between samples and between experiments were evaluated using statistical analysis.

**Specific Aim 2: To culture hMSC seeded fibrin microthreads for up to 7 days and evaluate cell growth, proliferation, and viability.**

The hMSC-seeded fibrin microthreads were cultured for up to 7 days and were quantified for cell growth at 3, 5 and 7 days. Hoechst staining was performed to view the cell distribution and growth on fibrin microthreads. At each of the above time points, hMSC cell proliferation and viability were assessed.



## Chapter 2: Background

The overall goal of the thesis project is to develop a new approach to developing a 3-dimensional (3-D) fully biologic tissue-engineered vascular graft. The specific emphasis of this thesis project was on developing an efficient and reproducible direct cell seeding technique that would allow cell attachment and growth on a tubular mandrel for vascular tissue formation. This section gives an overview of blood vessel structure and physiology, the clinical need for vascular grafts, current techniques to vascular graft tissue engineering, and the rationale for our approach.

### 2.1 Physiology and anatomy of a blood vessel

Arteries, veins and capillaries form the entire network of the circulatory system. The main function of arteries and veins is to transport blood throughout the body to and from the heart. In general, arteries carry oxygenated blood from the heart to the body and veins carry deoxygenated blood from the body to the heart. Both the arteries and veins have three distinct tissue layers (tunica) separated by layers of elastic fibers. The size and proportion of the outer two tissue layers in arteries vary with respect to their function and position, whereas the walls and innermost layer remains as a single layer of cells in all cases. In general, arteries are thicker, have more elastin compared to the veins, which allow the arteries to transport blood under high pressure. The three tissue layers are as follows:

- The **tunica intima** is made up of a single confluent layer of endothelial cells. It is surrounded by a basal lamina and connected to the internal elastic lamina. This layer helps in maintaining a thrombosis-resistant blood contacting barrier.
- The **tunica media** is the medial layer made up of smooth muscle cells interspersed in the matrix of elastic fibers, connective tissue and other ECM proteins. The medial layer gives

the vessel its elasticity and compliance properties. This muscular layer helps the artery to control blood flow through contraction and dilation.

- The **tunica adventitia** is the outermost layer made up of collagen, connective tissue and fibroblast cells. The main function of this layer is to provide mechanical strength to the vessel and protection to the inner layers.

## **2.2 Clinical significance**

Coronary artery disease (CAD) is one of the major forms of vascular diseases. According to the American Heart Association, approximately 17.6 million people suffer from CAD in United States alone with a mortality rate of approximately 10%. The annual expenditure on CAD is around \$177 billion[1]. These statistics show that CAD the most common and the most costly type of cardiovascular disease. It is caused due to the buildup of plaque inside the coronary arteries, a condition known as atherosclerosis.

Atherosclerosis is an inflammatory disease occurring as a result of the protective response to the damage done by the accumulation of fat along the vessel wall [18]. The disease begins with the damage to the innermost vascular layer made up of endothelial cells by oxidized cholesterol (low density lipoproteins) and eventually leads to thrombosis. Macrophages responsible for ingesting lipids are unable to breakdown oxidized lipids and in turn become foam cells at the site of fat accumulation. As more and more lipid accumulates the necrotic tissue at the core increases and over a period of time the tissue can calcify resulting in a hardened artery which is either partially or completely blocked. This results in obstruction or stopping of the blood flow through the vessel which can in turn result in a stroke.

## **2.3 Blood vessel replacements**

Percutaneous coronary intervention (PCI) and coronary artery bypass graft (CABG) surgery are the two widely used treatments for CAD, with the optimal treatment of the two still being a topic of debate [2-4]. Recent studies have supported the advancement of PCI with drug eluting stents as a promising treatment; however it is still restricted to some extent by restenosis, patient age and diabetic condition giving CABG a superior advantage [5,6,19,20]. In CABG surgery, the diseased vessels are replaced by the patient's own arteries or veins. The favorable choices of autologous vessel replacement are the saphenous vein or the internal mammary artery. However, autologous vessel replacement is not always the best option as it requires multiple surgeries and also increases patient risk and cost [21,22]. In certain cases, the patients' veins or arteries might not be healthy enough to act as replacement vessels or not enough replacement vessels are available due to previous surgeries [21]. This indicates the dire need to find alternate methods in order to substitute the diseased blood vessels.

### **2.3.1 Synthetic blood vessel substitutes**

Various approaches have been developed and tested to find a suitable blood vessel substitute. The early approach was to implant a synthetic biomaterial like polyethylene terephthalate (Dacron) or expanded polytetra-fluoroethylene (ePTFE). Although these synthetic biomaterials proved to be effective for large diameter blood vessels (>6mm) [7], they have failed in applications involving small-diameter blood vessels. For small-caliber arteries, they have demonstrated poor patency rates, primarily due to thrombus formation [9-11]. A six-year follow up study of ePTFE implantation for lower limb bypass surgery revealed acceptable immediate and short term patency rates, however the patency decreased to 20-30% after six years [23]. An

improvement to the problem of thrombogenicity with synthetic grafts was attempted by seeding a layer of endothelial cells onto these grafts. Although it was found that this approach improved patency and stability of the vascular grafts [24], the use of synthetic grafts still posed a problem of mortality and morbidity associated with graft infection and immunogenicity [8]. The results from implantation of unseeded and seeded synthetic grafts suggested a need for a better and more biocompatible vessel replacement.

### **2.3.2 Tissue engineered blood vessels**

To meet the need for vascular graft substitutes, researchers have turned to the approach of creating tissue engineered blood vessels (TEBV). Tissue engineering employs the principle of combining engineering techniques with the knowledge of biology in order to create a graft in vitro that mimics natural tissue structure and physiology. The advantages of using a biological TEBV is that in most cases there is no synthetic material involved, and hence there would be no foreign body reaction, no graft implantation infection, better biocompatibility and better patency rates. Implanting a TEBV is believed to encourage the host cells to remodel the matrix as required, in addition to the capacity of the TEBV grafts to self-renew [25,26].

Multiple experimental approaches to vascular graft tissue engineering have been reported; including implanting natural biomaterials (or decellularized tissues), seeding cells onto biodegradable scaffolds or seeding cells into biopolymer gels [12]. Weinberg and Bell were the first to attempt the approach of developing a TEBV. They cultured vascular cells in collagen gels to form the intimal, medial and adventitial layers, similar to a native blood vessel [14]. Although they were able to form these three-layered grafts analogous to native vessels, these grafts had weak mechanical properties. The grafts were not able to withstand high pressures and burst at

pressures as low as 10 mmHg. When provided with support sleeves made of Dacron, the mechanical strength of the graft was enhanced, but introduced the problem of using a synthetic scaffold. Since then, multiple attempts have been made at culturing cells in collagen gels and experimenting with methods to strengthen these gels, but a graft with mechanical strength comparable to native vessels still remain unrealized [27]. An alternate approach to TEBV is seeding cells into biodegradable scaffolds made of synthetic polymers such as polyglycolic acid (PGA). Niklason et al [13] tried seeding porcine aortic smooth muscle cells within a PGA mesh and cultured it under dynamic conditions for 8 weeks. They were successful in achieving high production of ECM proteins and burst pressures of 2000 mmHg. In vivo implantation showed positive results in terms of the feasibility of these vessels to sustain the mechanical environment of the arterial system [27]. However, there are issues regarding this approach. Firstly, there should be an optimal balance between matrix remodeling and scaffold degradation. There might be a possibility of the residual polymer in the final graft which may initiate a foreign body response. Also, the entire process of graft formation in vitro is 8 weeks long which might not be practical from the point of view of manufacturing cost. In addition, there might be a possibility of thrombosis with this approach due to inefficient endothelial layer formation. Recently, an alternate biodegradable polymer based on polyester urethane urea (PEUU) has shown promising results in the formation of a tissue engineered blood vessel [28-30]. However, the technique requires precise design of the scaffold for achieving the desired porosity and requires physical modifications to enhance cell attachment, mechanical strength and degradation [30]. Based on the arguments made until now, the studies show that there has been tremendous advancement in the field of TEBV. However, the most successful techniques demand complex design parameters in terms of selecting an optimal seeding mandrel, seeding or culture technique for cell

attachment and graft formation. Nevertheless, the concepts and techniques developed by these studies can form a platform for improvement in developing a simpler approach for creating TEBV.

### **2.3.3 Fully biologic tissue engineered blood vessels**

Recently, L'Heureux et al demonstrated a novel technique to develop vascular grafts, referred to as 'cell-sheet based tissue engineering' [15]. It is based on a fully biologic approach without the use of any exogenous scaffolds. Briefly, human vascular smooth muscle cells were cultured for 30 days to form a cell sheet which was then wrapped around a tubular mandrel to achieve the tubular morphology, acting as the medial layer. Similarly, a sheet of fibroblasts was formed and wrapped around the smooth muscle cell layer to form the adventitial layer. After allowing 8 weeks of maturation for the two layers, the mandrel was removed and endothelial cells were seeded along the lumen. The graft formation took approximately 3 months in total. The final graft showed high ECM production and matrix remodeling which is required for TEBV mechanical strength, suturability and compliance. The final graft exhibited burst pressure of 2000 mmHg (higher than human saphenous vein) and this mechanical strength was attributed to the collagenous matrix formation in the adventitial layer. Their results showed strong evidence that cells by themselves are capable of self-assembling, remodeling matrix and regenerating a new tissue that has a very close resemblance to a normal blood vessel. This technique is scaffold-free, which helps avoid the aforementioned problems associated with scaffold-based tissue engineering. However, the time required to manufacture this graft still poses a major hurdle in terms of clinical utility for emergency surgery and production cost. The technique also involves tissue manipulation in order to wrap sheets around the mandrel and to remove the mandrel.

Therefore, a simple and easy technique that would aid faster cell assembly and graft formation would help advance the concept of cell based tissue engineering closer to realizing a fully functional and clinically acceptable blood vessel.

## **2.4 Importance of cell seeding technique**

Direct cell seeding and growth on tubular mandrels may offer an alternative, totally biological approach to generating tissue engineered blood vessels. In this approach, cells are seeded directly onto a tubular mandrel, which act as an adhesive support. The technique allows the cells to self-assemble and remodel their own matrix to form a fully biologic tubular graft without the need to form and roll tissue sheets. The key to successful utilization of direct cell seeding is to allow maximum attachment of cells around the mandrel and facilitate cellular growth to form a tubular tissue.

Several techniques have been tried in the past to seed cells onto tubular scaffolds. Neumann et al [16] have tried direct seeding of rat aortic smooth muscle cells onto laminin-coated nylon strands which resulted in a 150  $\mu\text{m}$  thick tubular graft after 28 days of culture. In a similar approach for direct cell seeding, magnetic forces were applied around a tubular shaped collagen membrane [17,31] which encouraged the magnetically loaded cells to attach rapidly around the membrane with 90% seeding efficiency. However, the methods still need some degree of manipulation in mandrel removal or application of external forces to enhance cell attachment. Nevertheless, these studies demonstrate that devising an appropriate seeding technique would assist rapid cell attachment with maximum seeding efficiency and result in the desired tubular morphology.

### 2.4.1 Hanging drop seeding technique

A seeding technique with a similar concept to enhance cell attachment, and the current approach used by our lab is the hanging drop seeding technique. The schematic of a hanging drop technique is shown in Figure 2.

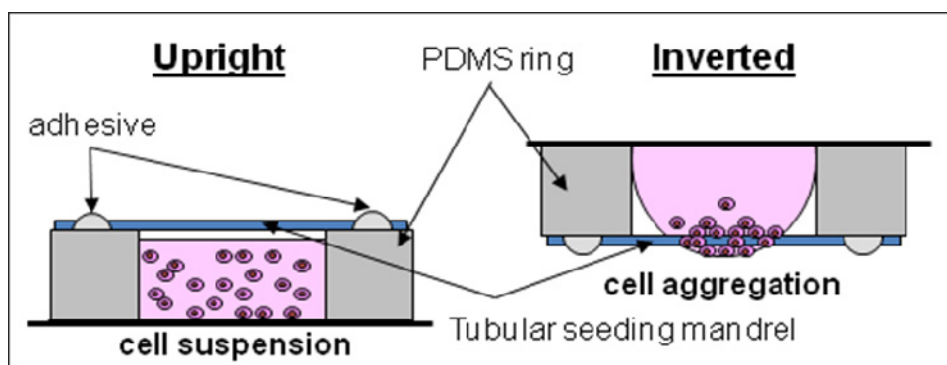


**Figure 2. Schematic of a hanging drop seeding technique [32]**

The method comprises a PDMS washer onto which a tubular seeding mandrel is glued using medical grade adhesive. Cell solution is pipetted into the cavity of the washer and the whole setup is then flipped upside down. During this hanging period, the cell solution forms a droplet around the seeding mandrel which in turn encourages the cells to attach to the mandrel. However, this technique has certain limitations pertaining to seeding consistency and reproducibility (see section 4.1) and involves complex setup requirements (see section 5).

### 2.4.2 V-shaped cell seeding chamber

Alternatively, we developed a simple seeding method that would allow rapid cell attachment in tubular fashion without involving any complex setup. We designed customized v-shaped cell seeding channels that would meet the aforementioned requirements. Figure 3 shows a



schematic of the v-shaped cell seeding chambers, depicting a tubular seeding mandrel and cells seeded on it.

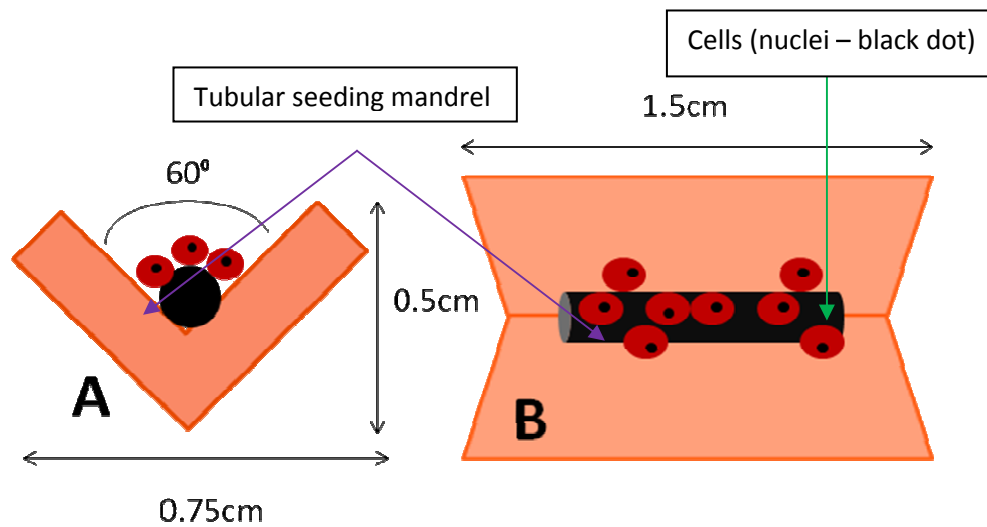


**Figure 3. Schematic of a v-shaped cell seeding chamber (A) Side view (B) Top view.**

Advantages of using these customized chambers are its shape and material. It is made from polydimethyl siloxane (PDMS) with the v-channel of the chamber made to just fit the tubular mandrel used for seeding. When the cells are seeded onto the mandrel in the chamber, they settle at the bottom of the v-channel due to gravity. As PDMS does not support cell adhesion, the cells have the only option to attach to the mandrel and nothing else. This enhances cell attachment using a simple method which is easy to set up with no complex procedures involved.

## **2.5 Bone marrow derived human mesenchymal stem cells**

Identification of the appropriate cell type and source is a critical factor for tissue engineering of blood vessels. Various cell types have been explored for seeding TEBVs. The ideal source of cells would be autologous vascular smooth muscle cells (SMC) and endothelial

cells (EC). A requirement for using autologous cells is to obtain a large number of cells from a biopsy sample of a patient. A study by Greiner et al [33] showed isolation of ECs, SMCs, and fibroblasts from a single vein biopsy but the quality of cells after expansion was questionable. Previous studies have shown that adult vascular cells have limited proliferation capacity and they start losing their function after a certain passage of expansion [34,35].

Alternatively, recent studies have suggested potential advantages of using mesenchymal stem cells (MSC) as a source of vascular cells for blood vessel tissue engineering. By definition, MSCs are multipotent stem cells that have the ability of self-renewal and differentiating into the mesenchymal, cardiomyogenic, myogenic, astrogenic and nerve cell lineage [36,37]. The various sources of the MSCs are the bone marrow, umbilical cord, placenta, peripheral blood, adipogenic or synovial tissue [38-40]. Of all these sources, bone marrow is the most commonly used source of the MSCs for tissue engineering as it yields a high count of the cells [41-43]. Hashi et al [44] seeded mesenchymal stem cells onto nanofibrous scaffolds made from poly L-lactic acid (PLLA). They found the grafts without MSCs showed intimal thickening and thrombus formation whereas MSC-seeded grafts had long term patency of up to 2 months in-vivo. This supports the fact that MSCs have antithrombogenic properties which is one of the crucial factors for a blood vessel. Also, the mesenchymal stem cells have the ability to differentiate into vascular smooth muscle cells [45]. A study by Galmiche et al demonstrated the ability of mesenchymal stem cells to differentiate into a vascular smooth muscle cells [46]. These reasons were the basis of our selection of human mesenchymal stem cells (hMSCs) as our seeding cell type.

## **2.6 Fibrin microthreads as tubular seeding mandrel**

Previous studies have reported the use of fibrin gels as scaffolds to assist cell seeding and matrix remodeling [47-50]. Bone marrow-derived mesenchymal stem cells have been shown to attach to fibrin gels [51,52]. Fibrin gels were used as a cell carrier for delivery of hMSCs and were determined to be biocompatible and had no adverse effects on cell growth, proliferation, migration and differentiation [49]. Recently, Cornwell demonstrated a novel approach to using fibrin as a scaffold for cell seeding and delivery [53] by creating microthreads from fibrin. Cornwell et al. found that the mechanical properties of fibrin microthreads were superior to those of fibrin gels. Given that these microthreads have a cylindrical shape allows the cells to grow in a tubular shape following cell attachment and proliferation. The microthread material and structure is conducive to cell attachment, proliferation and migration. In addition, it was found that the mechanical strength of the microthreads could be augmented by UV crosslinking, and that the increase in strength was proportional to the UV exposure time. This is advantageous in that it allows the control of the degradation rate of the fibrin microthreads by manipulating the UV exposure time. Depending on the required strength of the microthread during the cell seeding and culture period, the crosslinking exposure can be varied accordingly.

**Based on these arguments we decided to seed human mesenchymal stem cells onto fibrin microthreads using the v-well seeding technique and assess cell attachment, determine the consistency and reproducibility of the technique, and assess hMSCs growth and viability when cultured on fibrin microthreads.**

## Chapter 3: Materials and Methods

This section provides a detailed description of the various techniques, assays and approaches for cell culture and seeding, and quantifying cell number, proliferation and viability. The highlights of this section are a description of the two seeding methods used: 1) hanging drop [32] and 2) the newly developed v-shaped cell seeding approach.

### 3.1 Bone marrow-derived human mesenchymal stem cell (hMSC) culture

Bone marrow-derived hMSC (Lonza) were seeded in a 150 mm Petri dish at 5,000 cells / cm<sup>2</sup> in 20 ml of media. The cells were used between passages 7 to 11 for all studies. The hMSC were cultured in Mesenchymal Stem Cell Growth Medium (MSCGM) consisting of Mesenchymal Cell Growth Supplement (MCGS), L-Glutamine and GA-1000 (MSCGM™ BulletKit, Cat# PT-3001, Lonza). At 90% confluency, the cells were trypsinized using 0.25% trypsin EDTA solution (CellGro, Mediatech Inc) and a cell count was performed using the trypan blue exclusion method. A phase contrast image of passage 8 hMSCs in culture is shown in Figure 4 below.

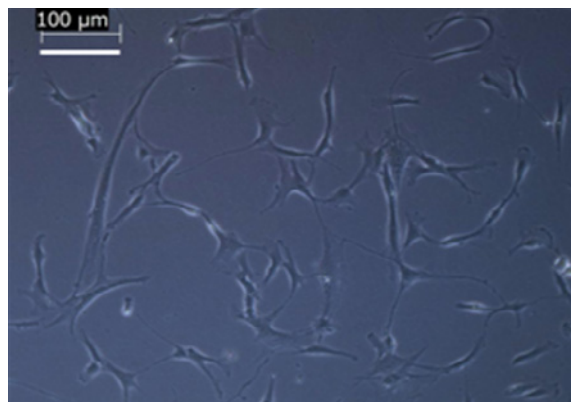


**Figure 4. Human mesenchymal stem cells in culture (passage 8)**  
**Image taken at a magnification of 20X. Scale bar = 100 microns.**

### 3.2 Production of fibrin microthreads

The fibrin microthreads were created using the protocol described in [53]. Briefly, 70 mg/ml of fibrinogen solution (Bovine plasma, Sigma, St Louis, MO F4753) was prepared in HEPES buffered saline (HBS, 20 mM HEPES, 0.9% NaCl). Thrombin (Sigma, St. Louis, MO T4648) was reconstituted at 6 U/ml in 40 mM CaCl<sub>2</sub> solution. The solutions were coextruded using a stabilized crosshead on a threaded rod with a crosshead speed of 4.25 mm/min through a blending applicator tip (Micromedics, St. Paul, MN) into polyethylene tubing with an inner diameter of 0.38 mm, and finally into a bath of 10 mM HEPES solution. A schematic of this process is shown in Figure 5.

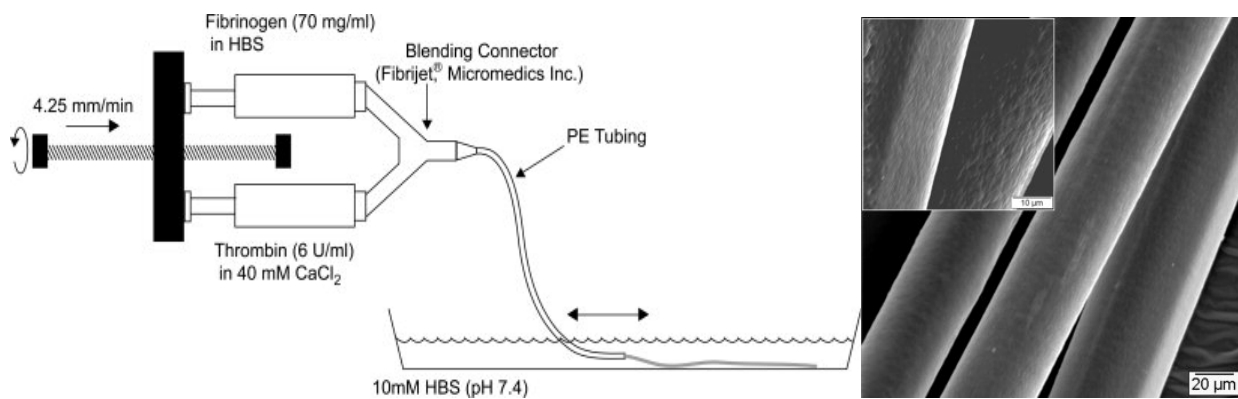


**Figure 5. Schematic of the extrusion of fibrin microthreads and scanning electron micrograph of the fibrin microthreads [53]**

Fibrin microthreads were removed from the bath suspended at their two ends and allowed to dry under the tension of their own weight. After drying, the microthreads were stored in a dessicator at room temperature until use. Using this extrusion technique, the average diameter of the microthreads in their hydrated state was 55-65 μm [53].

### 3.3 Cell seeding techniques

#### 3.3.1 Hanging drop cell seeding technique

This technique represents the current seeding method used in the lab for direct cell seeding onto tubular mandrels [32]. It was used as a standard for comparison for the new v-well seeding technique developed as a result of this thesis. The schematic of the hanging drop method is shown in Figure 6 below. The concept of this technique is to force cell attachment around a tubular mandrel by inverting a suspension of cells to form a hanging droplet so that cells concentrate by gravity at the bottom of the droplet, and near the surface of the seeding mandrel.

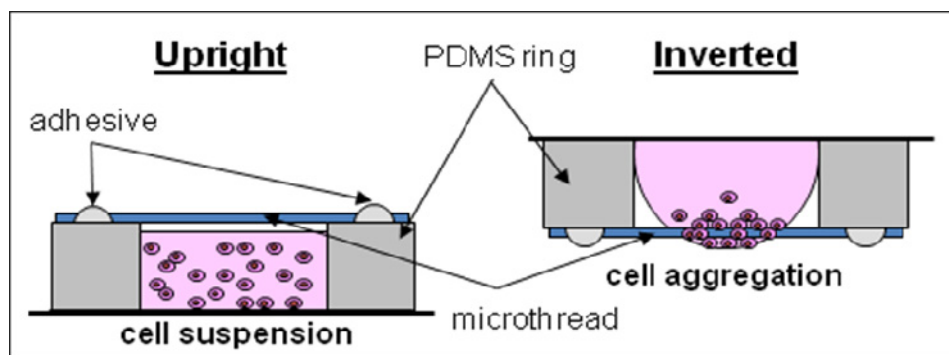


**Figure 6. Schematic of the hanging drop seeding method**

**A fibrin microthread is glued onto a PDMS ring and cells are seeded in the cavity. On inverting the sample, a hanging drop of cell solution is created which allows cell attachment due to accumulation of cells around the microthread.**

**Preparation of the PDMS ring** - The hanging drop seeding setup consists of a circular reservoir made from polydimethyl siloxane (PDMS; 184 Sylgard Silicone Elastomer kit, Dow Corning). PDMS is made by mixing silicone elastomer base and silicone elastomer reagent in a ratio of 10:1. The mixture is then degassed to get rid of any bubbles, poured into a 100 mm Petri dish and then cured in an oven at 60°C for 45 minutes to produce an approximately 0.5 cm thick PDMS sheet. A PDMS ring with a 1 cm inner diameter was then punched using a biopsy punch. The PDMS rings were then autoclaved for sterilization.

**Microthread assembly and sterilization** – A single fibrin microthread was glued onto the PDMS rings along the diameter using silicone medical adhesive (Silicone medical adhesive Type A, Dow Corning) such that the seeding length of microthread was 1cm. Figure 7 shows a fibrin microthread glued onto a PDMS ring.



**Figure 7. Image of a fibrin microthread glued onto a PDMS ring**

After allowing the glue to dry for 24 hrs, the microthreads were sterilized using a series of rinsing steps: 15 min PBS, 45 min 70% ethanol, 15 min PBS (3 times). Cell seeding was performed immediately following sterilization to avoid dehydration of the microthreads.

**hMSC seeding using hanging drop** - After the last rinse of PBS, hMSCs at a concentration of 50,000 cells per cm of microthread (100  $\mu$ l cell suspension; 500,000 cells/ml) were seeded into the PDMS ring. The PDMS ring along with the glued microthread and cell solution was then flipped upside down to achieve the hanging drop. The cells were seeded using the hanging drop technique for 4 hours after which the samples were flipped back to the upright position. The cell solution was aspirated and the sample was rinsed with PBS to get rid of any clinging or loosely attached cells. The fibrin microthread with the attached hMSCs was then subjected to analysis and characterization.

### **3.3.2 V-shaped cell seeding channels**

**Preparation of channels:** Polycarbonate molds machined in the shape of a pyramid served as a negative template. Polydimethyl siloxane (PDMS) was prepared as a mixture of silicone elastomer base and silicone elastomer curing agent in the ratio of 10:1. The PDMS was then degassed. The polycarbonate molds were glued on the inside of the Petri dish using silicone medical adhesive (Silicone medical adhesive type A, Dow Corning), with the apex of the molds facing up. The dish was then covered with the degassed PDMS such that the apexes of the molds were immersed into the PDMS. The setup was then heated in oven at 60°C for 60 minutes. The cured PDMS, along with the polycarbonate molds, was then removed from the Petri dish. The molds were removed manually and PDMS v-shaped channels remained Figure 8. The final dimension of the seeding chamber is 1.5 cm x 0.5 cm x 0.75 cm.



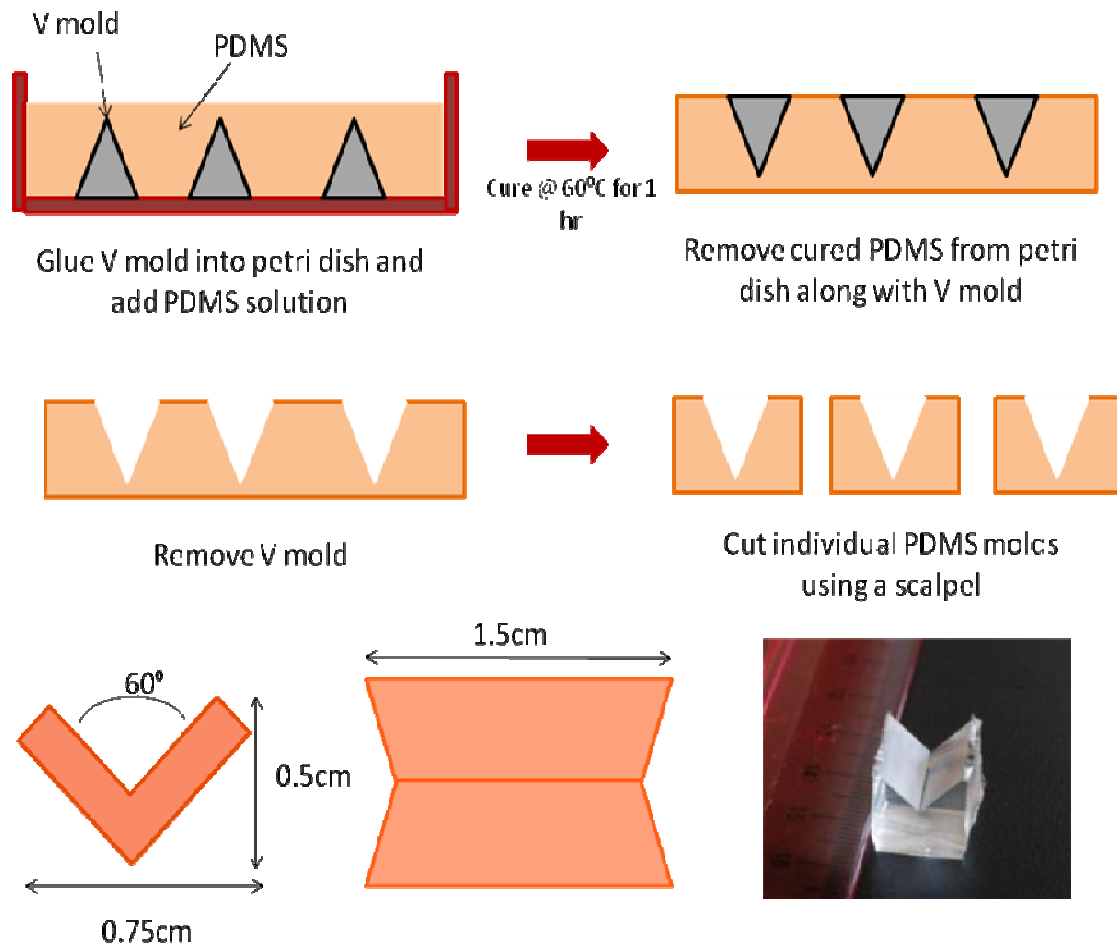


**Figure 8. Schematic showing the preparation and dimensions of the v-shaped PDMS chambers**

**Microthread sterilization and gluing:** The PDMS v-shaped channels were autoclave sterilized. A single fibrin microthread was then glued along bottom of the channel lengthwise using silicone adhesive (Silicone medical adhesive type A, Dow Corning) such that the seeding length of microthread was 1cm. It was important to make sure that the microthread was resting at the bottom of the channel before securing it in position using glue at the two ends. The glue was allowed to dry onto the microthreads in the channel for 48-72 hours. The microthread was then subjected to a series of rinsing steps for sterilization: 15min PBS, 45min 70% ethanol, 3 x 15min PBS. After sterilization, the microthreads were directly used for seeding without allowing them to dehydrate.

**hMSC seeding in v-shaped channels:** Human MSCs were trypsinized and resuspended at the required concentration of 50,000 cells in 100  $\mu$ l medium as described above. The PBS from the v-shaped channels was aspirated and 100  $\mu$ l of the hMSC solution was added to the channels, making sure the seeding volume is evenly distributed along the microthread length. The hMSCs were allowed to seed onto the microthreads for 4 hours at 37°C as shown in Figure 9. After 4 hours of seeding, the microthreads were analyzed for cell quantification and visualized for nuclei using Hoechst staining.

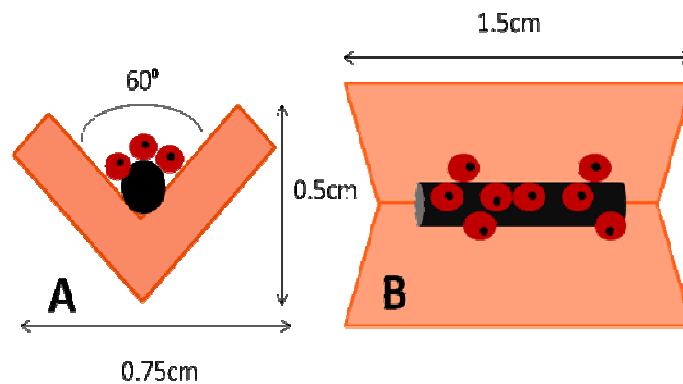


**Figure 9. Schematic of hMSC seeding onto fibrin microthreads in v-shaped PDMS chambers**

**Long-term culture in the v-shaped channels:** For long term culture, hMSCs were seeded onto fibrin microthreads for 4 hours as described above. The sample was then rinsed in PBS to wash off clinging and loosely attached cells. Each v-well sample was then secured into a well of a 6-well plate using sterile silicone vacuum grease (976V High vacuum grease, Dow Corning). Fresh media (7 ml) was then added into each well, making sure the sample was completely covered in media. The samples were then cultured for 3, 5 and 7 days. Media was changed every third day.

### **3.4 UV crosslinking of fibrin microthreads**

Fibrin microthreads were crosslinked as per the protocol described by Cornwell et al. [53] using a CL-1000 ultraviolet crosslinker (UVP, Upland, CA). The crosslinking device consisted of a bank of 5-8W UV tubes that produced radiation to crosslink the microthreads. Strands of microthreads were placed on a reflective surface of aluminum foil which was centered at a distance of 11 cm from the UV tubes. The exposure time was 20 minutes and hence resulted in a total energy of 8.5 J/cm<sup>2</sup> [53].

### **3.5 Characterization of cell attachment and distribution**

#### **3.5.1 Hoechst staining**

**Preparation of Hoechst dye.** To prepare the dye, 1.5 ml of distilled water was added to 5 µl of Hoechst 33342 reagent (Invitrogen) to get a final concentration of 33 µg/ml. The dye container was covered from light exposure until use.

**Staining:** The hMSC-seeded microthreads were removed from the seeding chambers at their respective time points using pointed forceps and scissors. They were thoroughly rinsed in PBS to get rid of any clinging or loosely attached cells. The microthread sample was fixed in 4% paraformaldehyde, then transferred onto a glass slide and stained with the Hoechst dye for 5 min, and protected from light during staining. After staining for 5 min, the Hoechst dye was removed and the microthread was washed with PBS three times. The microthread was mounted using a cover slip and mounting medium (Cytoseal, Cat#81678, Richard-Allan Scientific). Images were obtained using a Leica DM IL inverted fluorescent microscope in order to analyze the number of nuclei and morphology of attached cells.

### **3.5.2 Phalloidin staining**

In order to visualize the cytoskeletal organization of cells seeded on microthreads, cells were stained for F-actin using phalloidin. The samples (hMSC-seeded fibrin microthreads harvested at predetermined time points) were rinsed twice in PBS for 5 min. They were then fixed in 4% paraformaldehyde for 10 min. After fixation, they were rinsed twice in PBS for 5 min. The samples were permeabilized with 0.1% Triton X-100 in PBS for 10 min, then rinsed twice in PBS for 5 min. The samples were stained with Alexa 488-conjugated phalloidin (Cat# A11059 Invitrogen) for 30 min and covered from light. The samples were rinsed twice in PBS for 5 min and counterstained with Hoechst for nuclei visualization using the protocol described in 3.5.1. After Hoechst staining, samples were mounted on a slide and imaged under a fluorescent microscope. Images of nuclei and actin were acquired for each sample using an inverted microscope (Leica DFC420C), and individual images of the same microthread section were then merged using ImageJ to create a composite image.

### **3.6 Cell quantification - CyQuant NF**

The CyQuant NF assay (Invitrogen, Cat#C35006/C35007) was used due to its reported high sensitivity for quantifying cell numbers in the linear range of 20-20,000 cells. It is simple in that it does not require any washes, cell lysis or prolonged incubation. The working principle of the assay is that the CyQuant dye permeates through the cell membrane and binds to the DNA [54]. On binding to the DNA it emits fluorescence which can be measured. As DNA content represents cell number, this assay is effective for cell quantification from a sample and can be completed in as little as an hour.

**Protocol:** CyQuant NF dye solution – Prepare 1X HBSS buffer solution (component C, provided as 5X solution) in DI water. Add CyQuant NF dye (component A, provided as 500X solution) to

the 1X HBSS buffer solution such that the final dye concentration in the solution is 1X. Cover the conical tube with aluminum foil to avoid exposure to light. To determine the number of cells attached to fibrin microthreads, samples were removed from culture and rinsed twice in PBS to get rid of clinging and loosely attached cells. The rinsed samples were transferred to a 24-well plate containing 100  $\mu$ l 0.25% trypsin per well, making sure that each sample is completely immersed. Each sample was incubated in trypsin for 3 minutes. With trypsin treatment, cells were released, with simultaneous digestion of the fibrin microthread. An equal volume of media was then added to each well to neutralize the trypsin. The solution was mixed by trituration through a pipet to prepare a homogenous solution and was then transferred to a microcentrifuge tube and centrifuged for 5 minutes at 1,000 rpm to pellet the trypsinized cells. The supernatant was aspirated and 50  $\mu$ l of the CyQuant dye working solution was added to the cell pellet and mixed well. The 50  $\mu$ l solution was then transferred to a 96 well plate, in which each well corresponded to one trypsinized microthread sample. The plate was covered with aluminum foil to avoid exposure to light. The plate was incubated for 45-50 minutes at 37°C. A schematic of this method is shown in Figure 10.

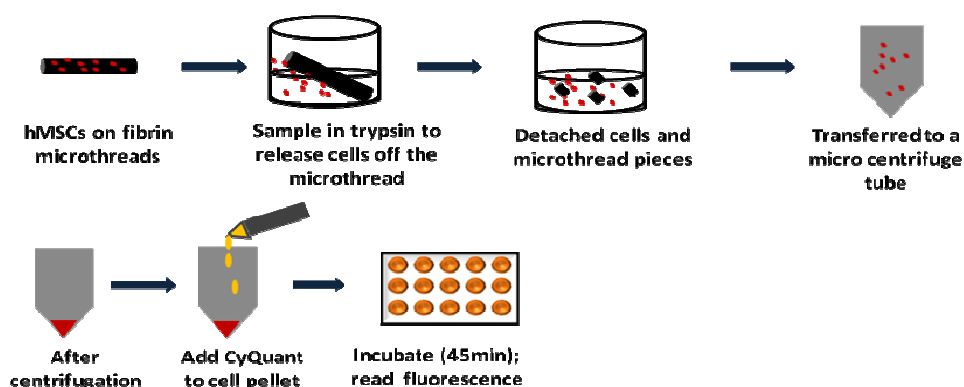


**Figure 10. Schematic of cell harvesting from fibrin microthreads and quantification of cell number using the CyQuant NF protocol**

After incubation, the fluorescence from individual wells was measured using a fluorescence plate reader (Victor3, 1420 Multilabel Counter, Perkin Elmer) at excitation/emission wavelengths of 485/520nm. The results were compared to a validated standard curve with cell range of 0-10,000 hMSCs in 1:2 serial dilutions Figure 11.

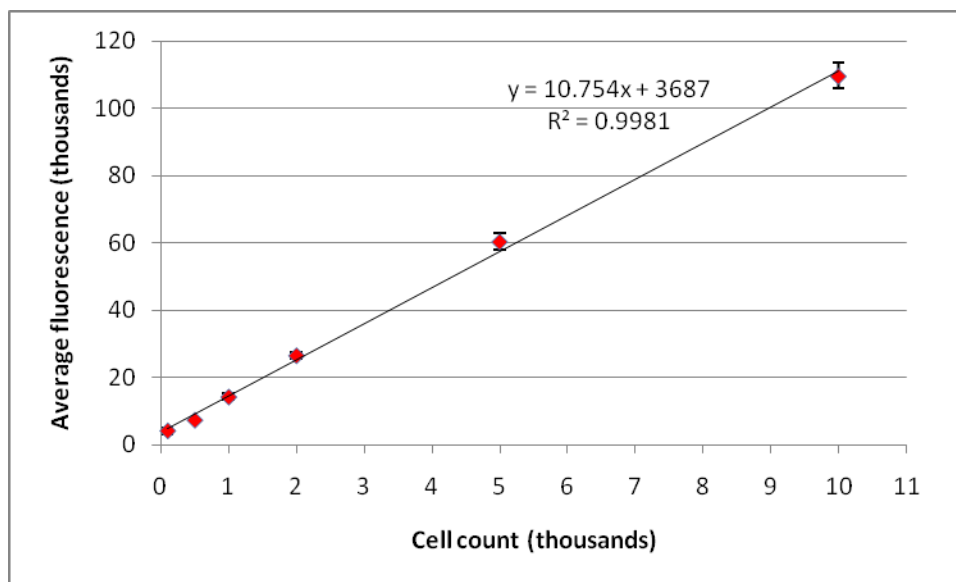


**Figure 11. Graph of the standard curve for CyQuant NF (n=3 for each cell concentration, black line – trend line)**

### 3.7 Cytotoxicity assay

In order to assess cell death on fibrin microthreads, the samples were stained using the LIVE/DEAD assay kit (Invitrogen, Cat# L3224) for mammalian cells. The kit consists of two fluorescent dyes – Calcein AM (green – 495/515 nm) and Ethidium homodimer-1 (EthD 1, red, 495/635 nm) that help distinguish the live cells from dead cells. The calcein is a cell permeant, naturally non-fluorescent dye which on entering live cells is enzymatically converted to a green fluorescent dye via esterase activity in live cells. The EthD 1 is able to permeate cells with

damaged membranes only, and binds with the nucleic acids to produce red fluorescence in dead cells. Hence, the viable cells stain green while the dead nuclei stain red.

**Protocol:** The stain is prepared by mixing 2  $\mu\text{m}$  of calcein AM and 4  $\mu\text{m}$  of EthD 1 in sterile PBS. Samples (fibrin microthreads with attached hMSCs) were washed with PBS for 5 min and were stained with the prepared LIVE/DEAD dye for 20 min at room temperature. During this period, the samples were protected from light. After staining, the samples were washed twice with PBS for 5 min. The samples were then loaded onto glass slides and fresh sterile PBS was added to keep them hydrated. Using a fluorescence microscope, images were taken of the red and green fluorescence and then merged using ImageJ. To quantify the percentage of dead cells, images of dead cells (red filter) were taken at various sections along the length of cell-seeded microthreads at the desired time points. Cells stained red (dead cells) were manually counted in each of these images where each image shows a microthread length of 400  $\mu\text{m}$ . Dead cells every 400  $\mu\text{m}$  of the microthread were averaged for four images per microthread to get average dead cells per 400  $\mu\text{m}$ . This average count was scaled to obtain the number of dead cells per cm of the microthread. The percentage of dead cells were calculated as the total number of dead cells normalized to the total cell count from the CyQuant NF cell quantification assay for that particular time point. The microthread samples used for viability assessment and CyQuant quantification are different samples but of the same group at the same time point. Images of live cells in the green fluorescent filter were also taken to confirm staining protocol and the presence of viable cells. An important note about the procedure of acquiring the images is that different images might represent different planes of the microthread as there is no way to ensure its consistency using the technique described. Plane of the microthread that gave optimal focus of microthreads and cells with minimal auto fluorescence was selected for imaging.

### 3.8 Click-it EdU cell proliferation assay

The Click-it EdU kit (Invitrogen, Cat# C10339) is a fluorescence-based assay for labeling DNA synthesis in proliferating cells. EdU (5-ethynyl-2'-deoxyuridine) is a thymidine analog which is incorporated into the DNA during active DNA synthesis. The protocol for the EdU detection assay is shown in Figure 12.

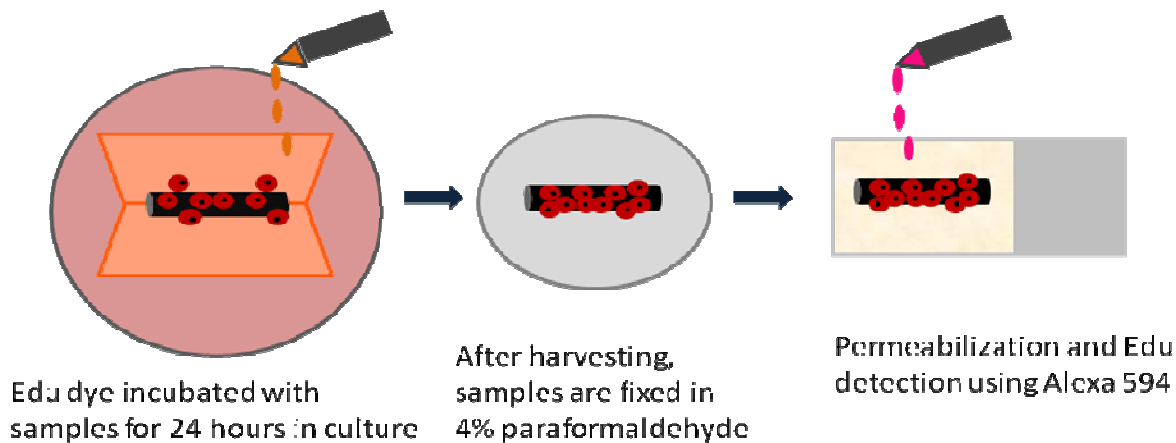


**Figure 12. Schematic of Click-It EdU cell proliferation assay**

The Click-It EdU cell proliferation assay was performed exactly as directed in the product manual. Briefly, 10  $\mu$ M EdU dye from a stock solution of 10 mM is added to the media while the samples are in culture. The dye was added to the cell culture media of the hMSC-seeded fibrin microthreads 24 hours prior to the desired time points to allow incorporation of the dye into the DNA of proliferating cells. After 24 hours of incubation, the media was aspirated and the fibrin microthread with attached hMSCs was transferred onto a glass slide. It was then fixed in 4% paraformaldehyde for 15 minutes at room temperature. The sample was then rinsed with PBS and permeabilized using 0.1% Triton X-100 in PBS for 15 minutes. After permeabilization, 500  $\mu$ l of Click-It EdU reaction cocktail was added to the samples and



incubated for 30 min at room temperature and protected from light. After incubation, the samples were washed with Click-It EdU rinse buffer and then mounted on a glass slide. Imaging was performed using the AlexaFluor 594 filter (excitation/emission wavelength of 590/615 nm). These samples were counter stained with Hoechst for nuclei visualization.

To quantify the percentage of proliferating cells, images of proliferating cells were taken at various sections along the length of cell-seeded microthreads at the desired time. Cells stained red (EdU-positive cells) were manually counted in each of these images where each image shows a microthread length of 400  $\mu\text{m}$ . Proliferating cells every 400  $\mu\text{m}$  of the microthread were averaged for  $n=4$  to get average proliferating cells per 400  $\mu\text{m}$ . This average count was scaled to obtain the number proliferating cells per cm of the microthread. The percentage of proliferating cells were calculated as the total number of proliferating cells normalized to the total cell count from the CyQuant NF cell quantification assay for that particular time point.

### **3.9 Statistical analysis**

Statistical analysis was done using Microsoft Excel. One way ANOVA was performed using  $\alpha = 0.05$ . The groups under analysis were considered to be statistically significant if  $p < 0.05$ . Every data set was expressed as mean  $\pm$  standard deviation. Type I errors were verified using Sigma Plot 11.0 analysis tool, where significantly different groups were subjected to Holm-Sidak post hoc analysis that was performed automatically post ANOVA analysis by the software. Holm-Sidak was appropriate in terms of comparing multiple independent groups for a significant difference and in controlling the family wise error (i.e. the probability of seeing Type I error). Also, as Holm-Sidak is less affected by statistical power as compared to the widely used Bonferroni correction, the dependence of results on number of groups compared reduces. Coefficient of variance (CV) was calculated as standard deviation \*100 normalized to cell count by

CyQuant NF. A statistical CV < 10% was considered as the allowable range of variance. A sample having a CV of < 10% for cell count was considered uniform and having an even distribution. Sample to sample variability having a CV < 10% was considered consistent and an experiment to experiment variability having a CV < 10% was considered reproducible.

### **3.10 Confocal imaging technique**

In order to assess cell attachment around the microthread circumference, images were taken using a confocal microscope (Leica TCS SP5 spectral confocal with a Leica DM16000 inverted research microscope) and z-stacks of confocal images were generated. Hoechst and phalloidin stained samples were mounted on glass slides and covered with a cover slip. The slide was then mounted onto the scope with the cover slip facing the lens. The focus was then adjusted to one plane within the visible cell layer which serves as one input range boundary. The focus was then adjusted to the other end of the visible cell layer which serves as the other input range boundary. A z-stack option is then selected wherein the microscope captures image slices between these boundaries with predetermined slice thickness. All these image slices are then stacked by the software (Leica LAS AF Lite) to generate a 3-D reconstruction of the cells on the fibrin microthreads.

### **3.11 Assessment of hMSC growth on fibrin microthreads in culture**

To measure cell growth on fibrin microthreads as a function of time in culture, we measured cell layer thickness from phase contrast images (pixel size of 1024 x 768) from each of three microthread samples (four phase contrast images per microthread) at every culture time of 3, 5 and 7 days. For each image, the side of the microthread which had thicker cell attachment was assumed to be the one exposed to cells during seeding. This side was designated as ‘Side 1’.

The side of the microthread that had fewer cells attached and hence showed less thickness (not exposed to cells during seeding) was designated as 'Side 2'. Using ImageJ, the cell layer thickness on either side of the microthread was quantified at five different points along the microthread in each image. Average cell thickness value was calculated for each microthread. Cell thickness was expressed as mean  $\pm$  S.D.

## **Chapter 4: Results**

This section focuses on the results and comparison of the hanging drop seeding technique and seeding using the v-shaped PDMS chambers. Each experiment included at least three samples per group. Cell attachment and distribution were assessed immediately after seeding or after up to 7 days in culture. Cell numbers were quantified by Hoechst nuclear staining and direct cell counting from fluorescent images and compared to quantification results using the CyQuant NF assay. Cell growth, viability and proliferation were quantified using CyQuant NF, CYQUANT NF/DEAD and Click-it EdU proliferation assays, respectively.

### **4.1 Comparison of hanging drop seeding and v-well seeding**

#### **4.1.1 Characterization of cell attachment and distribution by Hoechst imaging for hanging drop seeding**

Hoechst-stained fibrin microthreads seeded for 4 hours with hMSCs by the hanging drop seeding method are shown in Figure 13. Corresponding to every Hoechst image (Figure 13C, D), a phase contrast image was taken in order to visualize and compare the microthread morphology and orientation (Figure 13A, B). Images of Hoechst stained samples were taken at different regions along the length of each microthread in order to characterize hMSC attachment and distribution. Figure 13 shows cell attachment on fibrin microthreads after 4 hours of hanging drop seeding (Hoechst-positive nuclei in Figure 13D) compared to unseeded control microthreads (Figure 13B).

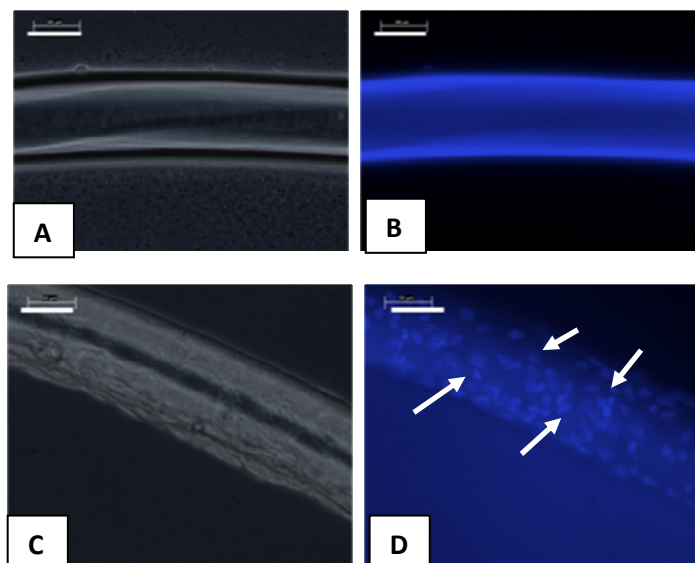


**Figure 13. Assessment of cell attachment by hanging drop seeding by Hoechst dye (A) Unseeded microthread as control (B) control stained with Hoechst (C) Fibrin microthread seeded with hMSCs using hanging drop (D) Hoechst image of the seeded microthread. Arrows point to the blue dots which are the nuclei of the attached cells (scale bar = 50 microns)**

Figure 14 (A-D) shows images from four different regions of a single fibrin microthread which was seeded with hMSCs for 4 hours. Cells appear to attach in clusters and do not appear to be evenly distributed along the length of the microthread. In addition, cell attachment varied from sample to sample. Average cell count by Hoechst stained images was  $396 \pm 404$  cells per cm of the microthread showing a CV of 102% (n=3 microthreads, four images per microthread).

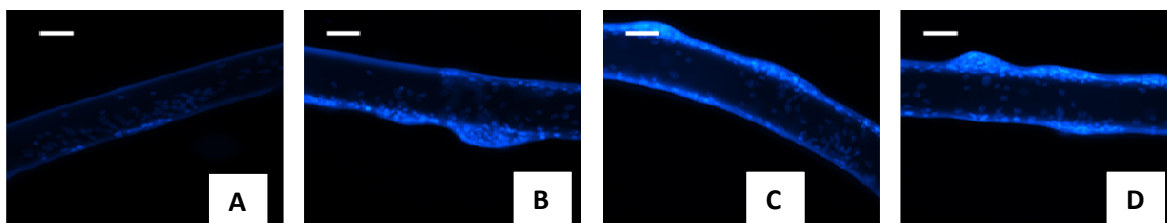


**Figure 14. Regions of an hMSC-seeded fibrin microthread after 4 hours of hanging drop seeding. The cell attachment is seen to be uneven and clustered along the length of the microthread (Scale bar = 50 microns)**

#### **4.1.2 Characterization of cell attachment and distribution by Hoechst and phalloidin imaging by v-well seeding**

As in the hanging drop cell seeding experiments, three samples of fibrin microthreads were seeded with hMSCs using the v-shaped chambers and phalloidin and Hoechst staining were performed. Images from different regions along the length of each microthread were acquired in order to assess the cell attachment and distribution, similar to the hanging drop seeding studies. Confocal microscopy was used to obtain images of different regions of a microthread sample and to visualize the two stains in the same image. The images are shown in Figure 15.

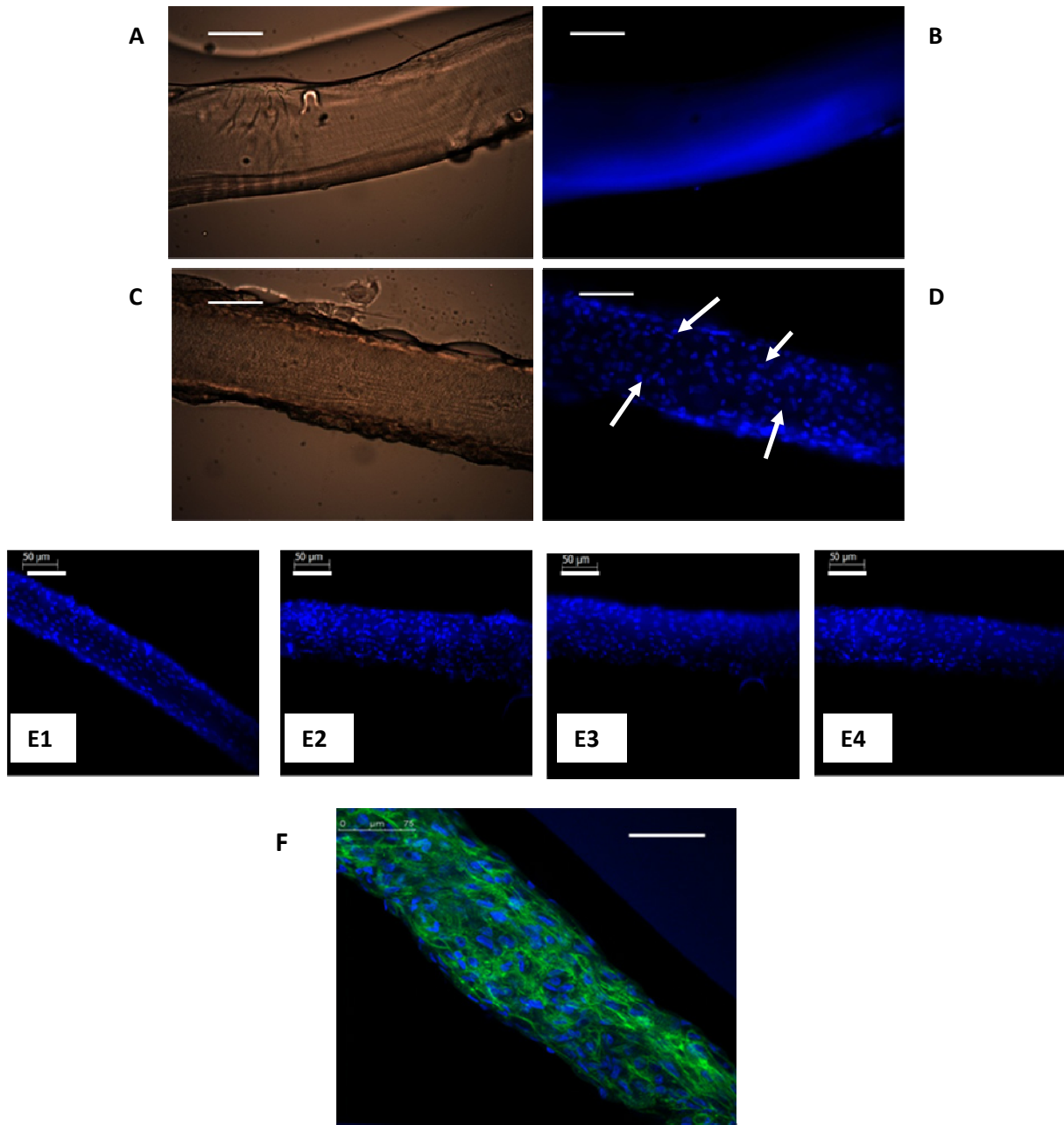


**Figure 15. Assessment of hMSC attachment in v-shaped chambers by Hoechst and Phalloidin**  
 (A, B) Phase contrast and Hoechst images of unseeded fibrin microthreads, (C, D) Phase and Hoechst image of a fibrin microthread seeded in a v-shaped chamber for 4 hours, (E1-E4) Hoechst images of four different regions of an hMSC-seeded microthread after 4 hours and (F) Confocal image of Hoechst and phalloidin. Arrows pointing at the blue dots represent few of the cell nuclei. Images acquired at 20X magnification. Scale bar = 50 microns

The Hoechst images of four different sections of the microthread as seen in Figure 15 (E1-E4) indicate that the cells are more evenly distributed along the microthread length. The count from Hoechst stained images was an average of  $5,680 \pm 850$  cells per cm of microthread with a CV of 15%. Also, there was no evidence of formation of clusters that was observed using the hanging drop seeding method (Figure 14). Phalloidin staining indicates complete coverage of the microthread by cells after only 4 hours of seeding Figure 15F.

#### **4.1.3 Comparing cell attachment using CyQuant NF assay for the two seeding methods**

CyQuant NF assay was used as an alternative method to quantify the number of cells attached on the fibrin microthread after 4 hours of seeding using the hanging drop method as well as the v-well seeding. Two experiments were performed with the exact same procedure for each of the respective seeding techniques. Three hMSC-seeded fibrin microthreads in each experiment were subjected to CyQuant assay. Figure 16 below shows the comparison of average cell count on fibrin microthreads from two experiments using the hanging drop and v-well seeding techniques.



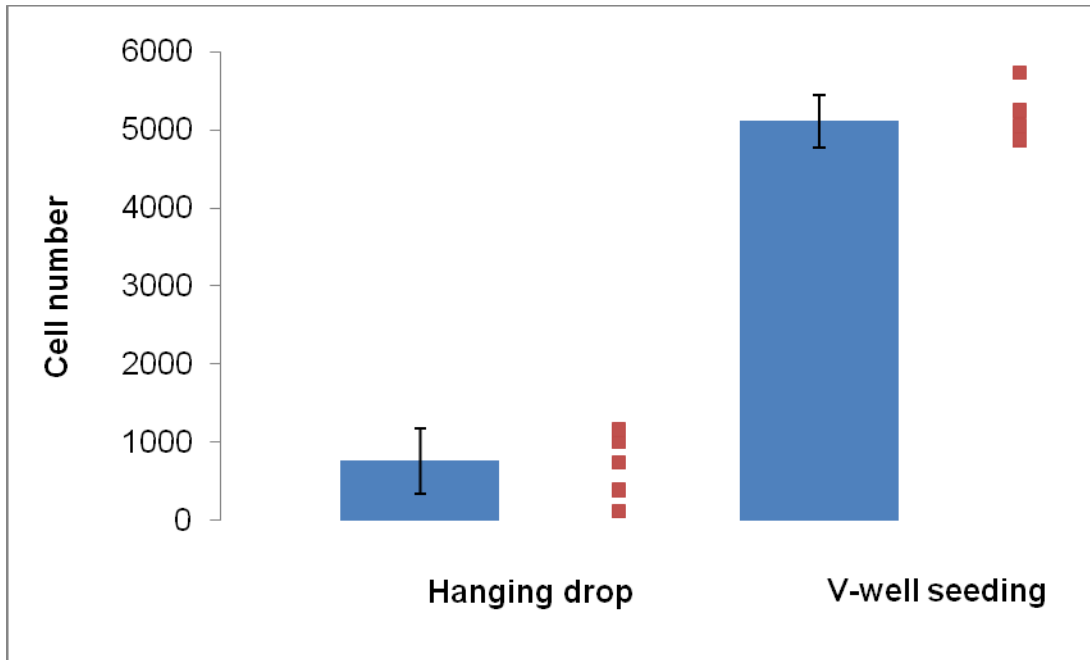


**Figure 16. CyQuant NF quantification of hMSC attachment by hanging drop and v-well seeding**  
**The blue bars represent the average number of cells attached to fibrin microthreads for each technique (n = 6; pooled from 2 separate experiments with n = 3 samples per experiment). The error bars show the standard deviation. The red squares represent the data points for each of the individual microthreads.**

The cell count from the first hanging drop experiment was  $964 \pm 193$  cells per cm of microthread, whereas the second experiment (using the same hanging drop protocol) resulted in  $564 \pm 538$  cells per cm of microthread. The two experiments combined showed an average count of  $764 \pm 422$  cells, as shown in Figure 16. The one-way ANOVA between the two experiments of hanging drop seeding resulted in a p-value of 0.29 ( $\alpha = 0.05$ ) indicating that average number of cells attached in each of the two experiments are not statistically different. In addition, samples within the same experiment demonstrated variable attachment suggested by the high CV of 20% in the first experiment, 95% in the second experiment and a combined CV of 55% and shown in Figure 16. This was also consistent with the clustered attachment observed from Hoechst images of fibrin microthreads seeded with the hanging drop seeding technique.

In contrast, the cell count from the first v-well seeding experiment was  $5,000 \pm 223$  cells per cm of microthread, whereas the second experiment (using the same protocol) resulted in  $5,228 \pm 445$  cells attached per cm of microthread. The two experiments combined showed an average count of  $5,114 \pm 339$  cells shown in Figure 16. The coefficient of variance observed in these experiments was 4% and 9%, respectively and a combined CV was 6.5%. One way ANOVA between the two experiments revealed a p-value  $>0.05$  which indicates that the means of the two experiments are not statistically significant.

Figure 16 (blue bars) suggests that the cell attachment by v-well seeding is approximately 6 fold higher than by the hanging drop seeding. The individual plot of each microthread for each of the two seeding techniques (red dots) suggest there is a higher sample-sample variability in cell attachment by hanging drop seeding as compared to cell attachment values seen among samples seeded with the v-well technique.

#### **4.1.4 Assessing cell viability with the CYQUANT NF/DEAD assay for v-well seeding**

As seen in Figure 17, samples were analyzed by CYQUANT NF/DEAD dye following a 4 hours seeding duration to evaluate the toxicity of seeded cells. The dead cells were counted as described in section 3.7. The dead cell count was expressed as a percentage of the total cell count determined by CyQuant analysis of microthreads seeded and harvested at the same time points. The mean cell count by CyQuant was 5,087 and the number of dead cells per cm of microthread was  $200 \pm 50$  giving a percent dead cell count of  $4 \pm 1\%$  at 4 hours post seeding.

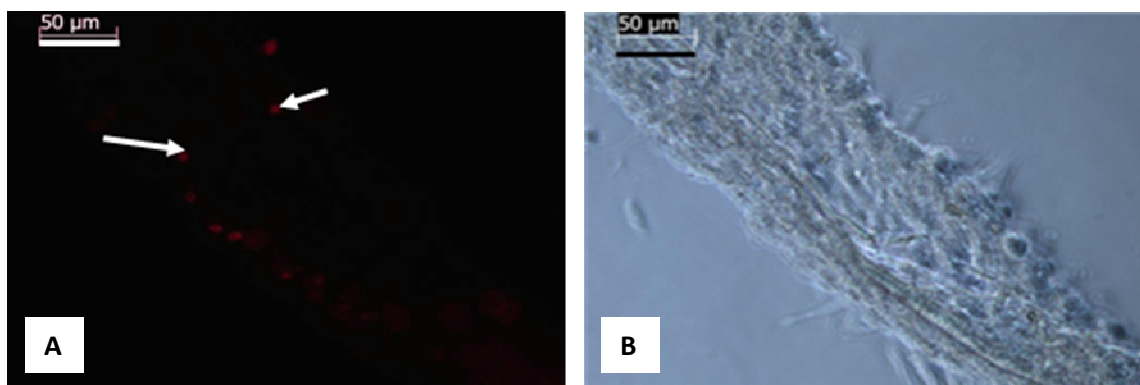


**Figure 17. Stained dead cells (A) and phase contrast image (B) of a fibrin microthread seeded with hMSCs for 4h. (Arrows indicate dead cells). 20X magnification. Scale bar = 50 microns**

## **4.2 Long term culture of hMSC seeded fibrin microthreads**

### **4.2.1 Characterization of cell attachment and distribution by Hoechst and phalloidin imaging**

After 3 days of culture, hMSCs on fibrin microthreads showed high levels of cell growth as seen in Figure 18, leading to breakdown in the microthread structure. The microthread no longer resembled a tubular shape and seemed to be partially disintegrated by the cells. After culturing the samples for 5 days, the fibrin microthread was no longer visible and appeared completely degraded by cells. While trying to pick up the microthreads from the v-shaped chambers after 5 days in culture, the microthread could not be distinguished from the cluster of cells. As the microthread could not be harvested in one piece, no data was obtained for hMSC-seeded microthreads at 5 days after culture and beyond.

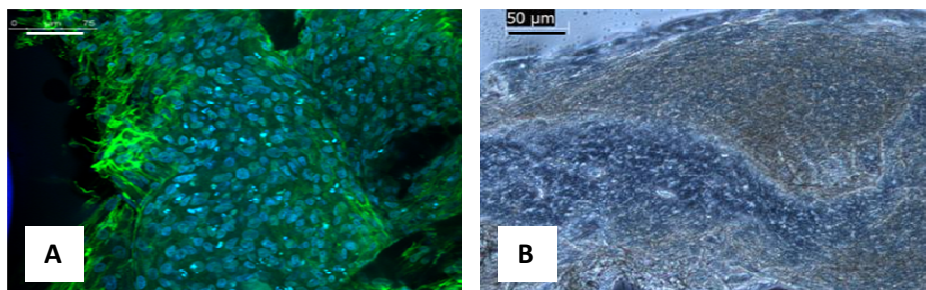


**Figure 18. Hoechst - phalloidin stained microthread (A) and phase contrast image (B) after 3 days cultured in v-well chambers. Microthread is degraded by the cells suggested by its weak mechanical structure. Images taken at 20X magnification. Scale bar = 50 microns**

#### **4.2.2 Quantification of cell attachment using CyQuant NF assay**

Three fibrin microthreads were seeded with hMSCs in the v-shaped chambers for four hours and then cultured for 3 days and cell number on the microthreads was quantified by CyQuant NF assay. The cell count from CyQuant after 3 days of culture was  $8,880 \pm 432$  cells per microthread, resulting in a coefficient of variance of 5% of the mean cell count.

#### **4.2.3 Assessing cell viability using live dead assay**

Three samples seeded for 4 hours and cultured for 3 days were analyzed by CYQUANT NF/DEAD dye to quantify cytotoxicity as seen in Figure 19. The average dead cells per cm of microthread were  $1,550 \pm 164$  cells. The quantity of dead cells, calculated as the percentage of the mean total cell count from CyQuant (which was 8,880 cells) was  $17 \pm 2\%$ . Even the image showing dead cells indicates that the microthread loses its structure after 3 days of culture and shows a large aggregate of cells (Figure 19-B). Analysis of further culture time points was not feasible due to degradation of fibrin microthreads by cells beyond 3 days.

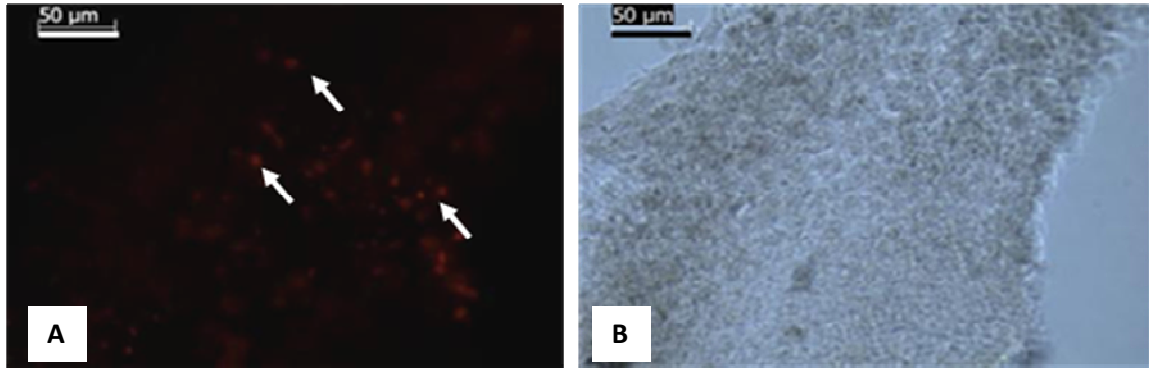


**Figure 19. DEAD staining of hMSCs (A) and phase contrast image (B) of microthreads in v-shaped chambers after 3 days (Arrows indicate dead cells) 20X magnification. Scale bar = 50 microns**

#### 4.2.4 Quantification of proliferating cells using Click-it EdU assay

The proliferating cells were counted from at least four images taken at various regions of every microthread sample as seen in Figure 20. Every image covered 400 µm of microthread, from which the average number of proliferating cells were counted. The proliferating cell count was expressed as a percentage of the mean total cell count determined by CyQuant (8,880 cells), which was  $7.32 \pm 1\%$  ( $650 \pm 100$  cells).

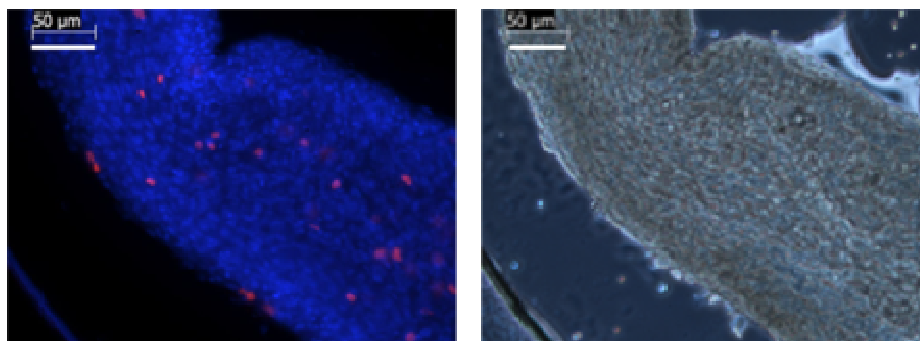


**Figure 20. Analysis of hMSC proliferation by Click-it EdU staining (A) and phase contrast (B) Fibrin microthreads were cultured with hMSCs in v-shaped chambers for 3 days. Pink dots represent nuclei of proliferating cells. Images taken at 20X magnification. Scale bar = 50 microns**

### **4.3 hMSC seeding on UV-crosslinked fibrin microthreads in v-shaped chambers**

Due to microthread degradation after 3 days of culture, microthreads were crosslinked by UV irradiation to decrease their degradation rate. The same cell seeding procedure was performed as described for hMSC seeding and culture of uncrosslinked microthreads. This section describes the results seen after 4 hours of hMSC seeding onto UV crosslinked fibrin microthreads in the v-shaped chambers.

#### **4.3.1 Characterization of cell attachment and distribution by Hoechst and phalloidin imaging**

The images in Figure 21 show that the hMSC attachment on UV crosslinked microthreads is similar to that of the uncrosslinked microthreads. Figure 21 (A, B) represent unseeded microthreads used as control samples. Figure 21 (C, D) are phase and Hoechst images respectively, of UV crosslinked fibrin microthreads seeded with hMSCs for 4 hours. The four Hoechst-stained sections of the sample in Figure 21 (E1-E4) show even cell attachment at different regions of the microthread. There is no evidence of formation of cell clusters after seeding. Figure 21F shows a confocal image of Hoechst and phalloidin staining.

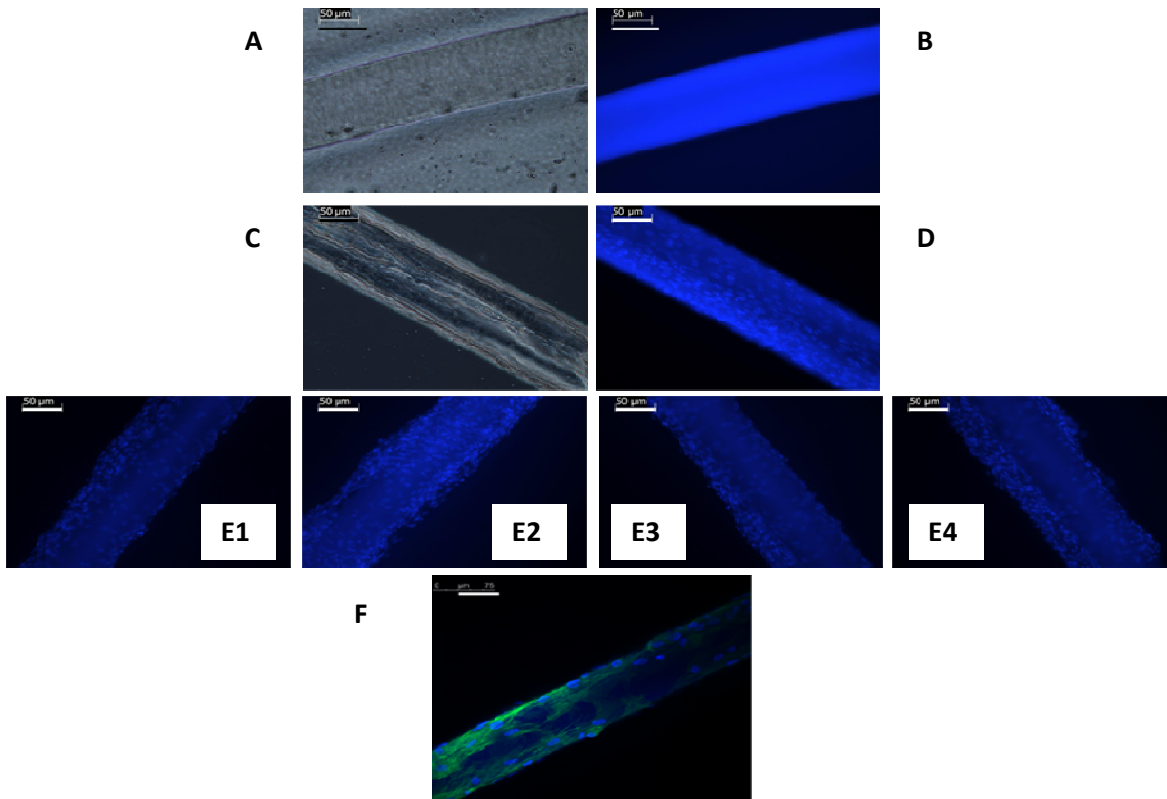


**Figure 21. Assessment of cell attachment on UV crosslinked fibrin microthreads shows unseeded UV crosslinked fibrin microthread phase contrast (A) and Hoechst (B) images and phase contrast (C) and Hoechst (D) images of UV crosslinked fibrin microthread seeded with hMSCs in v-shaped chambers for four hours, (E1-E4) Hoechst images of four different sections of a hMSC seeded UV crosslinked microthread after 4 hours and (F) Confocal image of sample stained with Hoechst and phalloidin. Images taken at 20X magnification. Scale bar = 50 microns**

#### **4.3.2 Quantification of cell attachment using CyQuant NF assay**

Three UV crosslinked fibrin microthreads seeded with hMSCs in the v-shaped chambers for four hours were quantified by CyQuant NF assay. The cell count by CyQuant was  $4,950 \pm 210$  cells that show a standard deviation of 4% within the sample group.

#### **4.3.3 Assessing cell viability via CyQuant NF/DEAD assay**

Three UV crosslinked fibrin microthreads seeded with hMSCs in the v-shaped chambers for four hours were quantified by CyQuant NF/DEAD assay for cytotoxicity and imaged as seen in Figure 22. The percentage of dead cells of the mean cell count by CyQuant was calculated.

The mean cell count by CyQuant was  $4,950 \pm 210$  cells per cm of microthread and the average dead cell number per cm of microthread was  $242 \pm 146$  cells, giving a percent dead cell count of  $5 \pm 3\%$ .

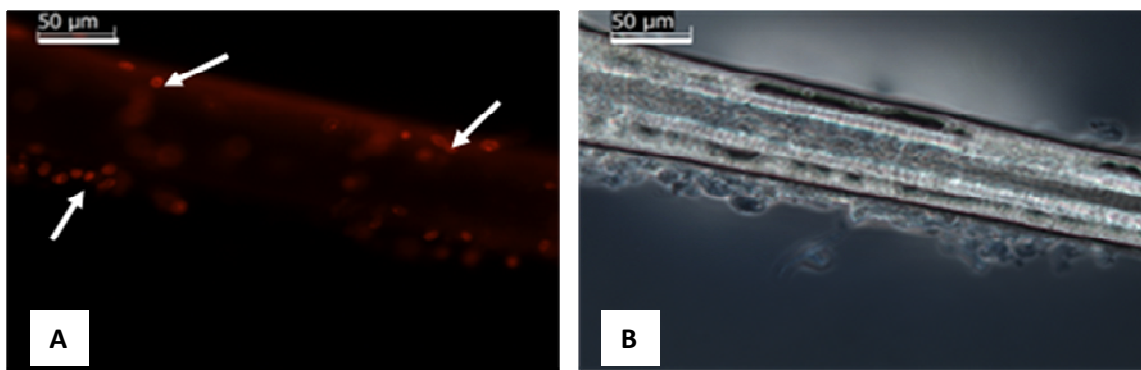


**Figure 22. DEAD cells on UV cross-linked fibrin microthreads (A) and phase contrast (B) seeded with hMSCs in v-shaped chambers for 4 hours. (Arrows indicate examples of dead cells). Images taken at 20X magnification. Scale bar = 50 microns**

#### **4.4 Long term culture of hMSCs on UV crosslinked fibrin microthreads**

##### **4.4.1 Characterization of cell attachment and distribution by Hoechst and phalloidin imaging**

After seeding for 4 hours, the attached hMSCs were allowed to culture on the UV crosslinked fibrin microthreads for 3, 5 and 7 days each. Three samples at each time point were co-stained with Hoechst and phalloidin to analyze cell attachment and distribution. The corresponding Hoechst and phase contrast images were merged using ImageJ to obtain a composite image. Phase contrast images were also taken for comparison. The images are as seen in Figure 23.



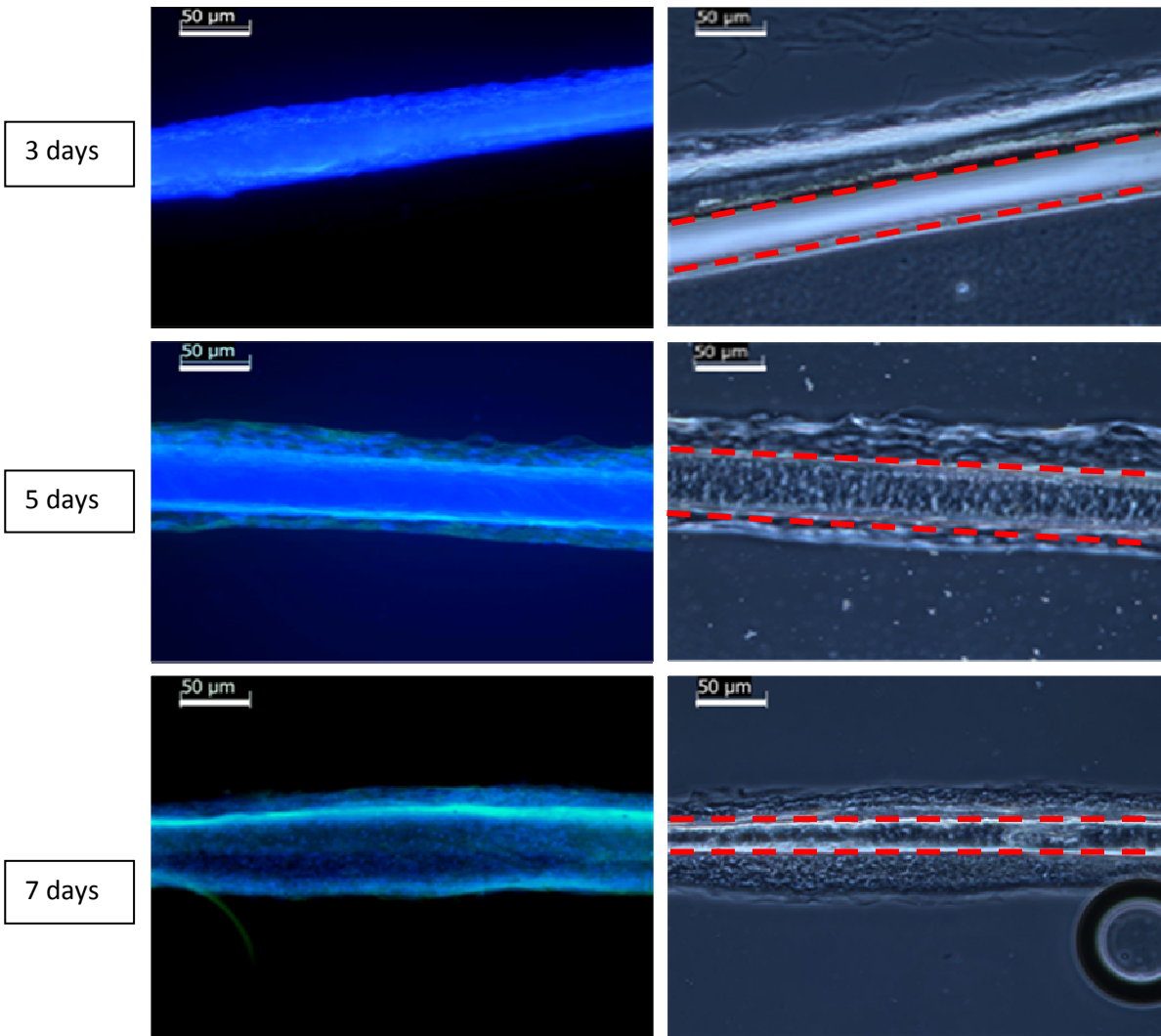


**Figure 23. Hoechst-Phalloidin merged (left) and phase contrast images (right) of UV cross-linked fibrin microthreads cultured with hMSCs for 3 days, 5 days and 7 days. Red dotted lines represent outer edges of microthread. Note the increase in thickness of cell layer below the bottom red line from day3 to day 7 in the phase images. Images taken at 20X magnification. Scale bar = 50 microns**

The Hoechst-phalloidin merged as well as phase contrast images show an increase in cell growth with the culture period. In figure 24, after 3 days of culture, we see that one side of the microthread appears to have fewer cells, similar to what is observed after 4 hours of seeding, and the hMSCs seem to be forming multi-layers which are thicker on one side than the other. After 5 days of culture, the cell growth on both sides of the fibrin microthread was observed in areas of the microthread which lacked cell attachment after seeding and 3 days of culture. There is a

simultaneous increase in the wall thickness observed by the increment in attached cell layers around the microthread. Eventually at 7 days, we observed that the microthread exhibits cell growth on all sides of the microthread.

The cell layers observed on both sides of the microthread suggested uniformity of cell growth along the circumference of the microthread. To quantify this, we calculated the thickness of the cell layers growing on each microthread as described in section 3.11. The two red dotted lines in each of the phase contrast images in Figure 23 represent the boundary of the microthread. The difference in the thickness of the two sides in the images of Figure 23 indicates that more cells may have attached on the side of microthread that was exposed to seeding (Side 1) compared to the other side of the microthread (Side 2). However, we do see an increase in the thickness of “Side 2” over the culture period as indicated by Figure 24. With time in culture, the difference in thickness between the two sides’ decreases and cell growth appears to become more uniform circumferentially.

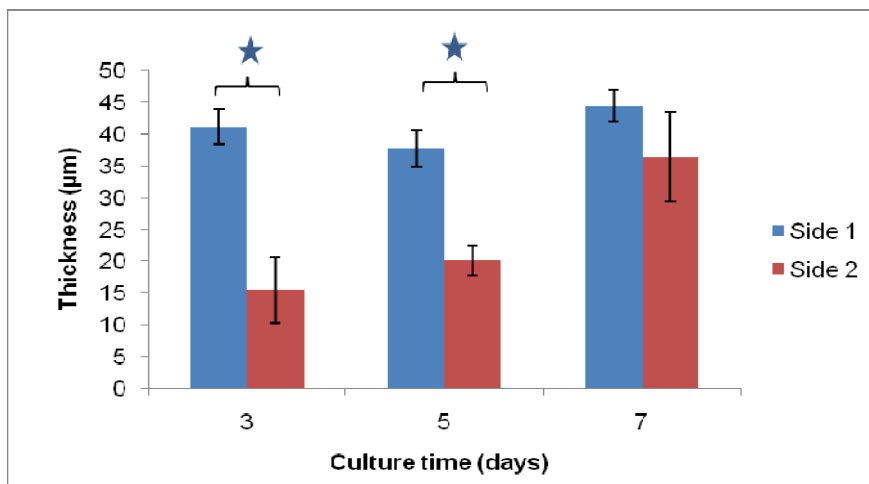


**Figure 24. Graph showing comparison of cell layer thickness**  
The difference in thickness of Side 1 and Side 2 is significant at day 3 and day 5 ( $p < 0.05$ ), whereas by day 7 the thickness of two sides become insignificant ( $p > 0.05$ ).  
( $n=3$  microthreads each time point, 4 images per microthread and 5 measurements per image on each side of the microthread) (★ = significantly different)

#### 4.4.2 Quantification of cell number as a function of culture time using CyQuant NF assay

Three samples at each culture period were assayed by CyQuant NF in order to quantify the number of cells per microthread at each time point. The average cell count and deviation were plotted for each time point and observed over the culture period, shown in Figure 25. We observed  $8,457 \pm 420$  hMSCs after 3 days in culture,  $10,066 \pm 669$  hMSCs after 5 days and  $11,198 \pm 582$  hMSCs after 7 days. The coefficient of variance observed were 5%, 7% and 5% respectively for each of these time points. One way ANOVA between the four time points gave a  $p < 0.05$  suggesting a 95% probability that the groups are not the same. Sigma Plot 11.0 performed the Holm-Sidak post hoc analysis which showed a  $p > 0.05$  suggesting there was a significant difference between each of the groups. These results are consistent with the images in the previous section which show an increase in cell number on fibrin microthreads as a function of time in culture.

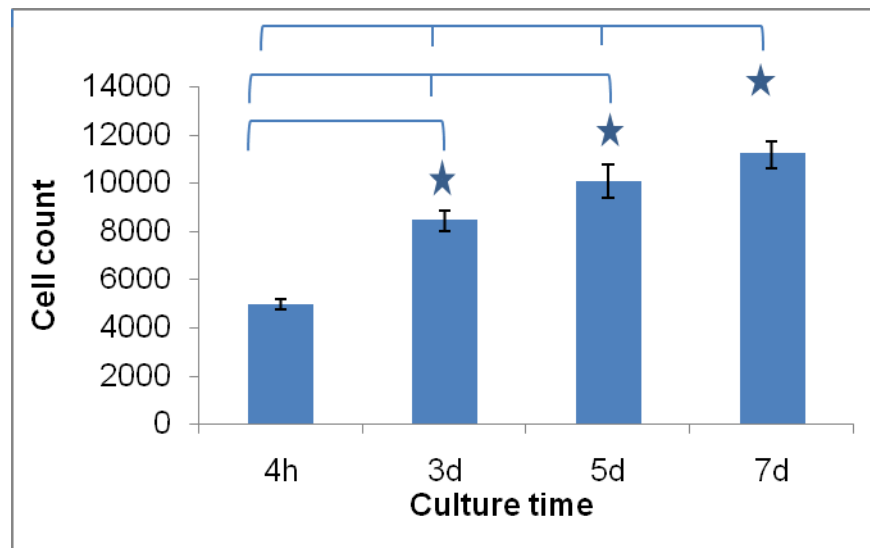


**Figure 25. Quantification of cells on UV crosslinked fibrin microthreads after 4 hours of seeding on fibrin microthreads followed by culture for 3, 5 or 7 days. Each bar represents mean +/- standard deviation (n=3 per time point). (\* = statistically significant from previous time point using One way ANOVA and Holm-Sidak post hoc analysis)**

#### **4.4.3 Assessing cell viability by CYQUANT NF/DEAD assay**

Three samples from each culture period were assessed for toxicity by CYQUANT NF/DEAD dye. At least four images along the microthread length were taken to quantify viability. Red nuclei (dead cells) were counted from each of the images and then averaged for the entire microthread. Percent dead cells were calculated as a fraction of mean cell count by CyQuant. Figure 26 (A, B, C) and Figure 27 below compares the percent of dead cells at the different culture periods.

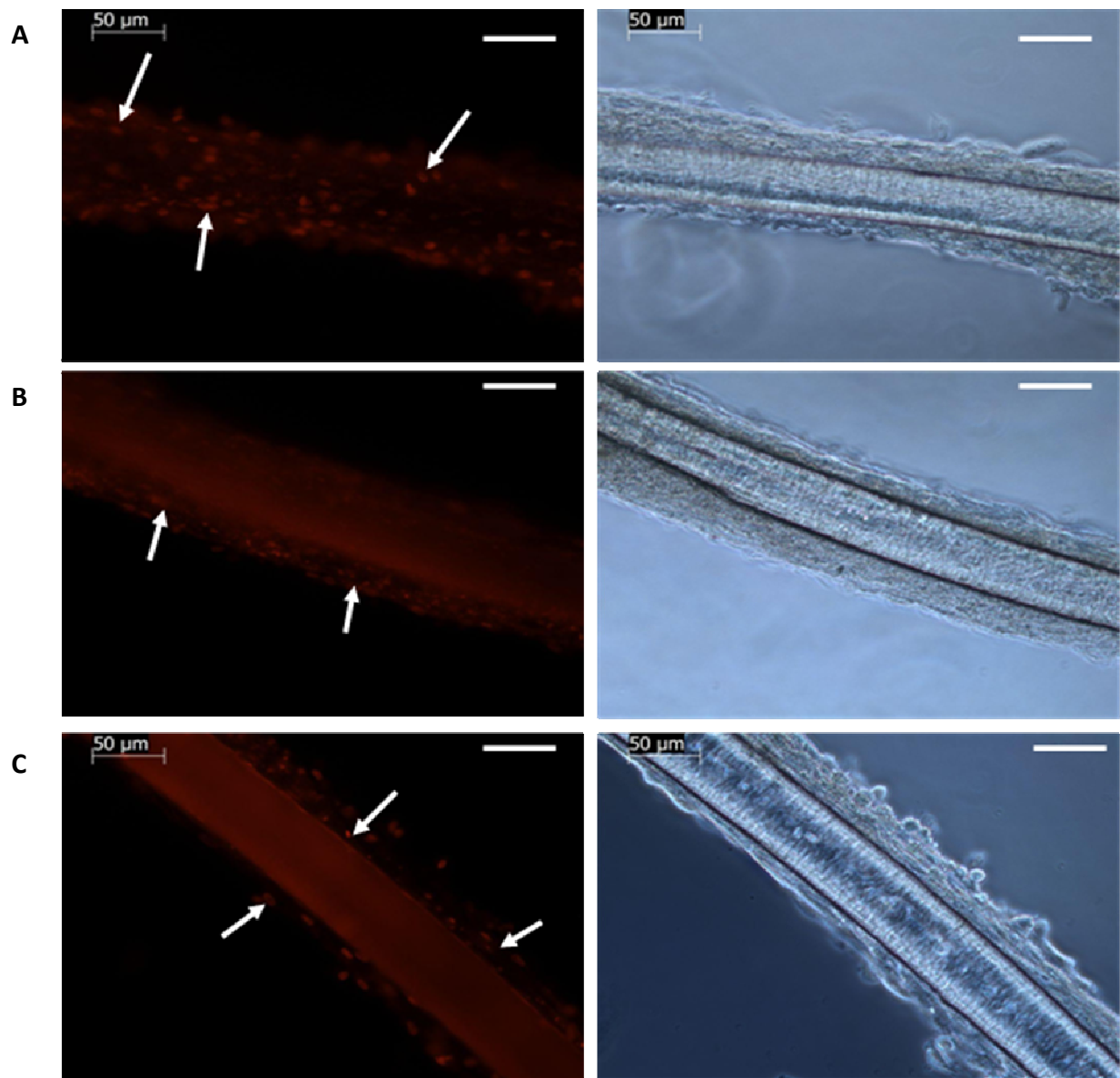


**Figure 26. DEAD cells on UV crosslinked fibrin microthreads and phase contrast images**  
**Microthreads were seeded for 4 hours and then cultured for 3 days (A), 5 days (B) and 7 days (C).**  
**(Arrows indicate example of the dead cells). Images taken at 20X magnification. Scale bar = 50**  
**microns**

The fraction of dead cells decreased as a function of culture period. At day 3 the percent dead cells was 24% which decreased to 15% at day 5 and 8% at day 7. One way ANOVA shows that dead cells decrease significantly from day 3 to day 5 ( $p = 0.0009$ ) and decreased

significantly further by day 7 ( $p = 0.0004$ ). This is evident from the number of red dots (that represent the nuclei of dead cells) that are seen in Figure 26 at each of the culture time points. This observation is shown in graph below in Figure 27.

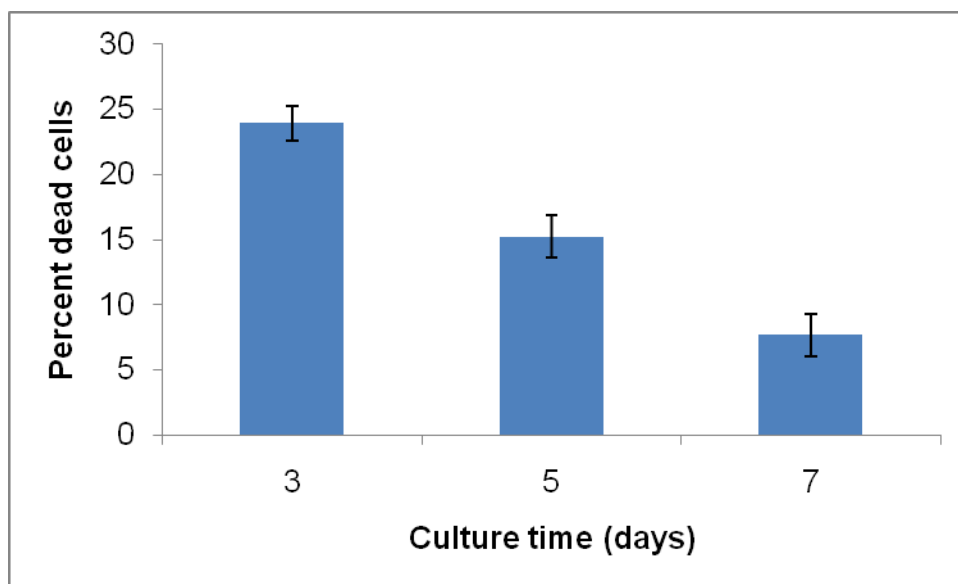


**Figure 27. Percentage of dead cells on UV crosslinked fibrin microthreads after 4 hours of seeding**  
**The microthreads were cultured for 3, 5 and 7 days. Each bar represents percent dead cells of that**  
**culture period with the error bar showing the standard deviation**  
**(n=3 samples for each experiment)**

#### 4.4.4 Quantification of proliferating cells using Click-it EdU assay

Three samples at each culture period were incubated with Click-it EdU dye for 24 hrs before their harvest. They were then co-stained with Alexa Fluor 594 conjugate and Hoechst dye to visualize attached nuclei and proliferating nuclei as seen in Figure 28.

We observe  $533 \pm 163$  EdU-positive cells after 3 days of culture (6.5% of total cell count), at day 5, there are no proliferating cells detected. At day 7, see  $583 \pm 126$  cells were EdU-positive, representing 5% of the total cell count. The data showed a coefficient of variance of 30% at day 3 and 21% at day 7.

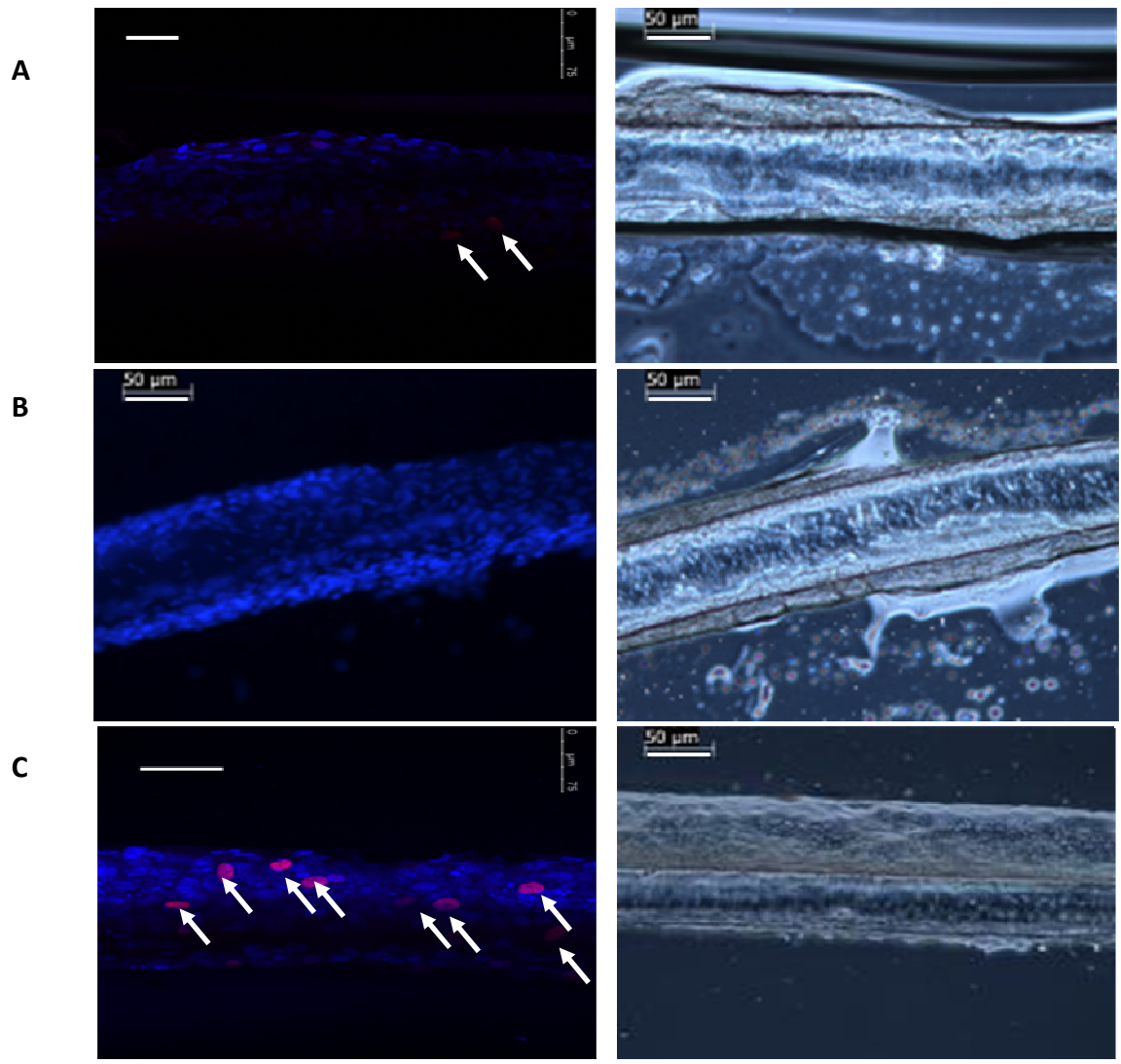


**Figure 28.** EdU-Hoechst stained images of UV crosslinked fibrin microthreads seeded with hMSCs. hMSCs were seeded on the fibrin microthreads for 4 hours and then cultured for 3 days (A), 5 days (B) and 7 days (C). Pink dots (with white arrows) represent nuclei of proliferating cells. Images taken at 20X magnification. Scale bar = 50 microns

## **Chapter 5: Discussion**

We were successfully able to develop a cell seeding and culture technique which allowed rapid attachment of human mesenchymal stem cells on fibrin microthreads after 4 hours of seeding. The technique supported growth and proliferation of the hMSCs on microthreads while maintaining their viability. This chapter discusses the advantages of using the v-shaped cell seeding chambers over the hanging drop seeding based on the results presented in Chapter 4. This chapter will also include a discussion of the results in the context of the project goals stated in Chapter 1.

### **5.1 Hanging drop seeding compared to seeding in v-shaped chambers**

Hanging drop seeding and seeding in v-shaped chambers are both based on a very simple concept of forced proximity of cells to a mandrel in order to achieve cell attachment. The hanging drop technique relies on the cells in the droplet attaching onto the fibrin microthread under gravity while in the inverted position. In contrast, in v-shaped chambers cells are allowed to settle at the bottom of the chamber under gravitational force where they interact with cell adhesive fibrin microthread and hence attach to them. The difficulty involved in setting up the sample in each method appeared to be major determining factors in the resulting cell attachment number, cell distribution along the microthread and variability of attachment quantity and distribution using each of these seeding techniques.

A comparison of cell attachment and distribution for the two seeding methods is shown by Hoechst images in Figure 14 and Figure 15E. Figure 14 shows different sections of a Hoechst stained sample that was seeded by hanging drop method and Figure 15E is of a sample seeded in v-shaped chambers. The hanging drop technique results in clustered attachment at random places



whereas seeding in v-shaped chambers results in non-clustered attachment. In addition, from Figure 14 we notice that the number of cells attached at different sections of the same microthread sample are variable, suggesting uneven distribution. On the other hand, Figure 15E shows highly even distribution of cells all over the microthread length, an indication of more uniform cell seeding in the v-shaped chambers. The observation of sample-sample variability by hanging drop within a group was confirmed by the CyQuant NF cell quantification assay. Figure 16 can be used as a comparison for cell attachment number between hanging drop seeding and seeding in v-shaped chambers. We observe that the hanging drop seeding experiments have a high CV of 55% in the two experiments combined (20% in experiment 1 and 95% in experiment 2). This suggests a high variability in cell attachment between samples of the same group. By seeding in v-shaped chambers the attachment data was observed to be consistent, demonstrated by a CV of 6.5% for the two combined attempts (4% in experiment 1 and 9% in experiment 2). This result suggests that the cell attachment after seeding in v-shaped chambers is more consistent from sample-sample and within acceptable limits of variability. The data also helps focus on the reproducibility of the seeding techniques. Statistical analysis by one way ANOVA between the two experiments with hanging drop seeding show a p value of 0.29 ( $\alpha = 0.05$ ). Statistically, the two experiments show no significant difference in cell attachment. Also, attachment by v-shaped seeding chambers shows a p value of 0.46. This p value suggests there is no significant difference between the two experiments performed by v-well seeding. However, due to a small sample size of  $n=3$  per group, there is a possibility of introducing a Type II error in performing ANOVA. As a result, we might not detect statistical difference despite a difference being present. A possible solution to avoid the Type II error would be to increase the sample size of the experiments. Finally, we also see a significant increase in the number of cells attached by

seeding in v-shaped chambers. There is an approximate 5-fold increase in cell attachment over hanging drop seeding, thus giving a higher attachment yield.

One of the major reasons for the hanging drop seeding producing sample and batch variability in results might be due to the difficulty involved in preparing the fibrin microthread seeding assembly. Figure 29 below depicts possible sources of error that might be introduced while gluing the fibrin microthread on a PDMS ring.

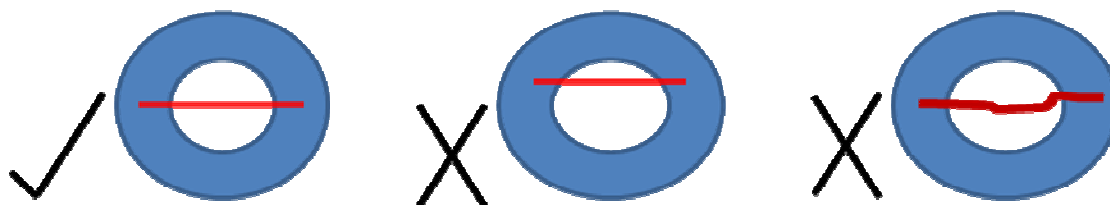


**Figure 29. Schematic of possible errors by hanging drop seeding**

The left schematic is the correct way of gluing the microthread straight across the PDMS ring diameter in order to get an ideal hanging droplet at the microthread. The middle and right schematics depict how erroneous gluing of microthreads could result in non-uniform hanging cell droplets in different samples and hence introduce variability in cell seeding in these samples. This may also result in unevenly distributed cells along the microthread length. Another possible source of error in hanging drop technique could be the manipulations involved in flipping of the sample upside down for achieving the hanging drop. The uncrosslinked fibrin microthreads are fragile and manipulating them in terms of gluing and flipping back and forth for seeding might induce additional stress, causing them to break. V-shaped chambers on the other hand have a simpler mechanism of sample setup allowing minimal manipulations. Simply gluing the microthread along the v-shaped channel of the chamber, without having to manipulate either the

microthread or the chamber, minimizes potential sources of sample preparation error which may contribute to more repeatable and reproducible cell attachment to fibrin microthreads.

## **5.2 Long term culture in v-shaped chambers**

Seeding with uncrosslinked fibrin microthreads in v-shaped chambers was effective in terms of rapid cell attachment and provided reproducible cell seeding results. However, long term culture with uncrosslinked fibrin microthreads proved to be problematic. After 3 days of culture, the Hoechst and phalloidin stained samples indicate that the fibrin microthread has completely lost its structural stability and eventually after 5 days it is completely degraded. At the end of 5 days we see a mass of cells with little evidence of the microthread. In order to form a tubular construct of cells around the microthread we needed to culture the samples for a longer period, for which we needed to increase the structural stability of the fibrin microthreads for them to sustain a longer culture period. Crosslinking the fibrin microthreads with UV radiation served this purpose.

### **5.2.1 Advantages of UV crosslinked fibrin microthread**

UV crosslinking of fibrin microthreads proved to be effective in enhancing the structural properties of the microthread. Cornwell et al [53] showed that UV crosslinking the fibrin microthreads increased their strength and stiffness and is dependent on the time and energy of exposure to the radiation. In another study by Cornwell et al [55], they have tried various crosslinking techniques with collagen microthreads, namely dehydrothermal treatment (DHT), UV crosslinking and carbodiimide (EDC) crosslinking. Of all the three, UV crosslinking was the simplest procedure and was effective in strengthening the microthread. Although it did reduce cell migration, they did not show any affect on cell attachment. The same was replicated by our studies where cell attachment before and after UV crosslinking was similar. In addition, we were

able to culture the hMSCs on these UV crosslinked fibrin microthreads for at least 7 days where the cells formed multi-layers, proliferated and were viable. UV radiation thus, proved to be a simple and effective choice for crosslinking the fibrin microthreads.

### **5.2.2 Cell attachment characterization**

Seeding hMSCs on UV crosslinked fibrin microthreads in v-shaped chambers did not result in any differences for cell attachment as compared to seeding on uncrosslinked fibrin microthreads. The Hoechst stained images of uncrosslinked and UV crosslinked fibrin microthreads demonstrate similar cell attachment and distribution along the microthread length. CyQuant NF cell quantification assay also suggests an attachment of approximately 5,000 cells on both, uncrosslinked as well as UV crosslinked fibrin microthreads. This is in confirmation with the results of Kevin Cornwell that UV crosslinking of fibrin microthreads does not affect cell attachment [53]. Dead staining too, showed a similar cell viability of 96% and 95% for uncrosslinked and UV crosslinked fibrin microthreads respectively. This was an additional confirmation that cell seeding is not affected by crosslinking.

Long term culture of attached hMSCs on the UV-crosslinked fibrin microthreads in the v-shaped chambers demonstrates growth of cells over time. Phalloidin stained samples show an increase in cell number (or increase in wall thickness around the microthread) resulting in multi-layers. CyQuant NF assay reconfirms the growth of cells over culture period from 8,500 cells at day 3 to 11,200 cells at day 7. A drawback or a shortcoming of this technique could be the fact that after seeding, cells attach only on the side of the microthread that was exposed to cells during seeding. As a result we see a thick cellular layer on one side of the microthread than the other, until day 3 (where it is prominent) and day 5 (where the difference in thickness reduces). The side of the microthread (Side 1) which was exposed to seeding shows a consistent thickness

of about 40  $\mu\text{m}$  from day 3 through day 7. Side 2 shows an increase in thickness from  $15 \pm 5 \mu\text{m}$  at day 3 to  $36 \pm 7 \mu\text{m}$  at day 7. The p values from one way ANOVA show that the difference in cell layer thickness of the two sides are significantly different from each other at day 3 and day 5 ( $p < 0.05$ ). The difference is not significant by day 7 ( $p > 0.05$ ). This reduction in difference of thickness on the two sides suggests that the cell growth is trying to establish uniform coverage on either side. This data supports the fact that cells have a tendency to grow towards the unexposed surfaces in order to form a uniform cell growth, presumably around the microthread. Although the data helps in determining hMSC growth towards unexposed surfaces and formation of multi-layers, there are a couple of technical limitations to this approach. Firstly, measuring thickness on either sides of microthread makes it difficult to accurately understand circumferential coverage of microthread by cells. Secondly, it is difficult to analyze the same two sides of the microthread consistently in different images as was in the case of dead staining protocol described in section 3.7. An alternative approach where we could analyze the increase in entire circumferential thickness consistently during culture could be useful. Confocal microscopy may help address this limitation.

Cytotoxicity assay showed a high percentage of dead cells at day 3 (24%) which decreases over culture period to 15% at day 5 and 8% at day 7. This may be attributed to the medium change cycles (media change every 3 days) as one of the possibilities. The samples at day 3 are analyzed for toxicity with medium changed just post seeding, whereas for day 5 samples the medium is changed two days prior to analysis (day 3 post seeding) and for day 7 samples the medium is changed only one day prior to analysis (day 6 post seeding). The more recent the medium change, the healthier the cells may be and fewer dead cells may be observed. Another possibility for reduced toxicity over culture period could be the fact that the cells are

recovering from the initial stress due to seeding, rinsing and also adjusting to the new environment. Since the percentage of viable cells is high, we can say that the cells appear to be growing normally. Click-it EdU proliferation assay shows around 6.5% proliferating cells at day 3, no proliferating cells at day 5 and 5% at day 7. A repeat experiment showed the same trend of no proliferating cells at day 5 and approximately same percent of proliferating cells on day 3 and day 7. However, not enough experiments have been performed with Click-It EdU to analyze the cell proliferation in order to get a conclusive data. The absence of proliferating cells on day 5 could be attributed to the medium change schedule. As medium is changed every third day for the samples, the samples analyzed on day 5 were fed with new media on day 3 (2 days prior to their analysis) and injected with EdU dye on day 4 (24 hours prior to analysis). During this period of 24 hours before EdU incubation, the medium might be used up by the cells and when the dye is introduced it might not detect any cells in proliferative phase. Cornwell et al [53] have stated in their study that cell proliferation reduces on crosslinking the microthread. However, when compared to percent proliferating cells attached on uncrosslinked fibrin microthread after day 3 (7.3%), it is not a significant difference. On the other hand, Hoechst stained samples and CyQuant NF assay suggest a growth of cells over culture period that does not seem to correlate well with the number of proliferating cells observed. One of the possible reasons could be the inability of the EdU dye to penetrate the thick cell layer and detect proliferating cells close to the microthread surface. It might be detecting proliferating cells only on the outer surfaces of attached cell layers.

When we compare our results to a similar seeding technique employed by Neumann et al [16] where they seeded aortic SMCs on nylon strands, they were able to form a 70-100  $\mu\text{m}$  thick SMC layer around the strand in 21 days revealed from histological sections. Analysis of cell

layer thickness by ImageJ and phase contrast images show that we have achieved cell layer attachment amounting to a thickness of roughly 45  $\mu\text{m}$  after 7 days of culture for one of the sides, while the other side shows a gradual increase in thickness trying to cope up with the former side. They use a seeding density of 3,000 cells per  $\text{mm}^2$  which is almost the same as ours, 2,702 cells per  $\text{mm}^2$ . Regarding the seeding efficiency, there have been related studies that have seeded cells onto tubular mandrels and have achieved >95% seeding efficiency [31,56]. Comparatively, we seeded 50,000 cells per cm of microthread and achieved an attachment of roughly 5000 cells, indicating a seeding efficiency of about 10% which is considerably lower. However, it is important to note that the studies so mentioned have used a different cell source and a seeding mandrel which is not degradable which is what we are aiming. In addition, the most important factor contributing to a higher seeding efficiency is that they employ a rotational seeding technique as opposed to our static seeding, which allows for a complete circumferential attachment during seeding. A similar idea can be employed in v-well seeding technique in order to achieve a complete circumferential attachment which will be discussed in Chapter 6.

## **Conclusions**

The goal of this project was to develop a simple cell seeding technique that would allow rapid cell attachment to a tubular mandrel with reproducible results and minimal sample manipulation. V-shaped cell seeding chambers helped us achieve hMSC attachment in as short as 4 hours. There was minimal sample-sample variability shown by a CV of 6.5% which is within the acceptable range of consistency which was set as 10%. Also, batch-batch variability represented by a p value of 0.46 between the experiments show that the means of the two experiments are not significantly different. This confirms that the technique is reproducible. It involved no complex sample setups and manipulations to achieve the effective seeding. UV crosslinking helped the fibrin microthreads maintain their mechanical integrity for at least 7 days without compromising hMSC attachment and further allowed for hMSC growth, proliferation and viability through that 7 day culture period. We were also able to demonstrate that hMSCs tend to form multi layers around the fibrin microthread over the culture period. A difference in thickness of cell attachment after day 3 which reduces significantly after day 7 suggests the hMSCs tend to form a uniform coverage on either sides of the fibrin microthread.



## **Chapter 6: Future work**

We were able to develop a novel cell seeding technique using the v-well chambers and seeding human mesenchymal stem cells onto fibrin microthreads in those chambers. The technique allowed for rapid and uniform cell attachment of hMSCs which showed growth, viability and proliferation through 7 days of culture, post seeding. However, there still remains a scope for improvement in the v-well seeding technique which might be incorporated as future work to this project. In addition, this chapter also discusses some key studies that would help take this project a step closer to the general goal of developing a fully biologic tissue engineered tubular cell construct.

### **6.1 Monolayer cell attachment post-seeding**

Seeding hMSCs on fibrin microthreads in the v-wells showed the cell attachment predominantly on the surface of microthread that was exposed to cell seeding, referred to as top layer here. While, the bottom layer showed minimal cell attachment immediately after seeding suggesting that cells only attached to the top layer of the thread, whereas the bottom part in the v-well is not accessible for cell seeding. A solution to this problem could be the flipping of microthread post seeding and repeating the seeding process. As a result, the unseeded surface of the microthread will now get cell attachment during the second seeding. Although this will double the total seeding time to 8 hours, but will result in complete circumferential cell attachment as opposed to attachment on only one surface.

## 6.2 hMSC characterization

In addition to smooth muscle cells, the mesenchymal stem cells have shown to differentiate into fat and bone [51,57-60]. It would be highly undesirable for the hMSCs to differentiate into any of these lineages if our primary concern is to eventually use these hMSCs as smooth muscle cells. In order to make sure that hMSCs have maintained their pluripotency, before going further with a longer culture study, it would be beneficial to characterize the attached hMSCs after 7 days of culture in v-wells.

Differentiation of hMSCs towards the adipogenic and osteogenic lineages can be verified using commercially available kits that provide with adipogenic and osteogenic induction medium. In order to detect for their differentiation, hMSCs from the 7 day cultured samples can be stained with Oil red O for adipogenic differentiation and Alizarin red S for osteogenic differentiation [61]. Negative controls can be developed by culturing hMSCs in adipogenic and osteogenic induction medium and then staining these cultured cells with the respective dyes. A positive control would be hMSCs that are grown in tissue culture dishes and then stained with the same protocol as negative controls. If the hMSCs cultured in v-wells have maintained their multipotency, they would stain negative for lipid vacuoles and calcium deposition. An alternative approach of characterizing hMSC pluripotency could be performing immunofluorescent staining with surface markers. Negative markers for MSCs like CD14, CD45, CD34 and positive markers CD29, CD73, CD105 and CD90 have been widely used and can be employed for our study too [36,57,62,63].

### **6.3 Longer hMSC culture on fibrin microthreads in v-wells**

Once the hMSCs have been confirmed for their pluripotency, it would be useful to culture them longer on fibrin microthreads using the v-wells. After 7 days of culture studies as described above, we witnessed cell growth, proliferation and viability while the UV crosslinked fibrin microthread still maintained its structural integrity. This encourages us to conduct further culture studies for cell growth, viability and proliferation analysis on the microthread. Formation of a tubular cell construct with increasing wall thickness, strength and compliance with simultaneous degradation of the fibrin microthread would be an ideal situation. Analysis of culture samples at regular time points for these parameters will help in developing optimal conditions for formation of the desired tubular cell construct.

## References

- 1 Lloyd-Jones D, Adams R, Brown T, Carnethon M, Dai S, De Simone G, Ferguson T, Ford E, Furie K, Gillespie C, Go A, Greenlund K, Haase N, Hailpern S, Ho P, Howard V, Kissela B, Kittner S, Lackland D, Lisabeth L, Marelli A, McDermott M, Meigs J, Mozaffarian D, Mussolino M, Nichol G, Roger V, Rosamond W, Sacco R, Sorlie P, Stafford R, Thom T, Wasserthiel-Smoller S, Wong N, Wylie-Rosett J: Executive summary: Heart disease and stroke statistics--2010 update: A report from the american heart association. *Circulation* 2010;121:948-954.
- 2 Barner H: Status of percutaneous coronary intervention and coronary artery bypass. *Eur J Cardiothorac Surg* 2006;30:419-424.
- 3 Hlatky M, Boothroyd D, Bravata D, Boersma E, Booth J, Brooks M, Carrié D, Clayton T, Danchin N, Flather M, Hamm C, Hueb W, Kähler J, Kelsey S, King S, Kosinski A, Lopes N, McDonald K, Rodriguez A, Serruys P, Sigwart U, Stables R, Owens D, Pocock S: Coronary artery bypass surgery compared with percutaneous coronary interventions for multivessel disease: A collaborative analysis of individual patient data from ten randomised trials. *Lancet* 2009;373:1190-1197.
- 4 Mehta R, Lopes R, Ballotta A, Frigiola A, Sketch MJ, Bossone E, Bates E: Percutaneous coronary intervention or coronary artery bypass surgery for cardiogenic shock and multivessel coronary artery disease? *Am Heart J* 2010;159:141-147.
- 5 Klein L: Are drug-eluting stents the preferred treatment for multivessel coronary artery disease? *J Am Coll Cardiol* 2006;47:22-26.
- 6 Loop F, Lytle B, Cosgrove D, Stewart R, Goormastic M, Williams G, Golding L, Gill C, Taylor P, Sheldon W: Influence of the internal-mammary-artery graft on 10-year survival and other cardiac events. *N Engl J Med* 1986;314:1-6.
- 7 Drury J, Ashton T, Cunningham J, Maini R, Pollock J: Experimental and clinical experience with a gelatin impregnated dacron prosthesis. *Ann Vasc Surg* 1987;1:542-547.
- 8 Mertens R, O'Hara P, Hertzner N, Krajewski L, Beven E: Surgical management of infrainguinal arterial prosthetic graft infections: Review of a thirty-five-year experience. *J Vasc Surg* 1995;21:782-790; discussion 790-781.
- 9 Abbott W, Megerman J, Hasson J, L'Italien G, Warnock D: Effect of compliance mismatch on vascular graft patency. *J Vasc Surg* 1987;5:376-382.
- 10 Ao P, Hawthorne W, Vicaretti M, Fletcher J: Development of intimal hyperplasia in six different vascular prostheses. *Eur J Vasc Endovasc Surg* 2000;20:241-249.

- 11 Tiwari A, Salacinski H, Punshon G, Hamilton G, Seifalian A: Development of a hybrid cardiovascular graft using a tissue engineering approach. *FASEB J* 2002;16:791-796.
- 12 Patel A, Fine B, Sandig M, Mequanint K: Elastin biosynthesis: The missing link in tissue-engineered blood vessels. *Cardiovasc Res* 2006;71:40-49.
- 13 Niklason L, Gao J, Abbott W, Hirschi K, Houser S, Marini R, Langer R: Functional arteries grown in vitro. *Science* 1999;284:489-493.
- 14 Weinberg C, Bell E: A blood vessel model constructed from collagen and cultured vascular cells. *Science* 1986;231:397-400.
- 15 L'Heureux N, Pâquet S, Labbé R, Germain L, Auger F: A completely biological tissue-engineered human blood vessel. *FASEB J* 1998;12:47-56.
- 16 Neumann T, Nicholson B, Sanders J: Tissue engineering of perfused microvessels. *Microvasc Res* 2003;66:59-67.
- 17 Perea H, Aigner J, Hopfner U, Wintermantel E: Direct magnetic tubular cell seeding: A novel approach for vascular tissue engineering. *Cells Tissues Organs* 2006;183:156-165.
- 18 Noll G: Pathogenesis of atherosclerosis: A possible relation to infection. *Atherosclerosis* 1998;140 Suppl 1:S3-9.
- 19 Lemos P, Hoye A, Goedhart D, Arampatzis C, Saia F, van der Giessen W, McFadden E, Sianos G, Smits P, Hofma S, de Feyter P, van Domburg R, Serruys P: Clinical, angiographic, and procedural predictors of angiographic restenosis after sirolimus-eluting stent implantation in complex patients: An evaluation from the rapamycin-eluting stent evaluated at rotterdam cardiology hospital (research) study. *Circulation* 2004;109:1366-1370.
- 20 Smith SJ, Dove J, Jacobs A, Kennedy J, Kereiakes D, Kern M, Kuntz R, Popma J, Schaff H, Williams D, Gibbons R, Alpert J, Eagle K, Faxon D, Fuster V, Gardner T, Gregoratos G, Russell R: Acc/aha guidelines of percutaneous coronary interventions (revision of the 1993 ptca guidelines)--executive summary. A report of the american college of cardiology/american heart association task force on practice guidelines (committee to revise the 1993 guidelines for percutaneous transluminal coronary angioplasty). *J Am Coll Cardiol* 2001;37:2215-2239.
- 21 Ratcliffe A: Tissue engineering of vascular grafts. *Matrix Biol* 2000;19:353-357.
- 22 Schmidt C, Baier J: Acellular vascular tissues: Natural biomaterials for tissue repair and tissue engineering. *Biomaterials* 2000;21:2215-2231.
- 23 Charlesworth P, Brewster D, Darling R, Robison J, Hallet J: The fate of polytetrafluoroethylene grafts in lower limb bypass surgery: A six year follow-up. *Br J Surg* 1985;72:896-899.

- 24 Williams S, Rose D, Jarrell B: Microvascular endothelial cell seeding of eptfe vascular grafts: Improved patency and stability of the cellular lining. *J Biomed Mater Res* 1994;28:203-212.
- 25 Hoerstrup S, Zünd G, Sodian R, Schnell A, Grünenfelder J, Turina M: Tissue engineering of small caliber vascular grafts. *Eur J Cardiothorac Surg* 2001;20:164-169.
- 26 Thomas A, Campbell G, Campbell J: Advances in vascular tissue engineering. *Cardiovasc Pathol* 2003;12:271-276.
- 27 Nerem R, Seliktar D: Vascular tissue engineering. *Annu Rev Biomed Eng* 2001;3:225-243.
- 28 Guan J, Sacks M, Beckman E, Wagner W: Synthesis, characterization, and cytocompatibility of elastomeric, biodegradable poly(ester-urethane)ureas based on poly(caprolactone) and putrescine. *J Biomed Mater Res* 2002;61:493-503.
- 29 Guan J, Fujimoto K, Sacks M, Wagner W: Preparation and characterization of highly porous, biodegradable polyurethane scaffolds for soft tissue applications. *Biomaterials* 2005;26:3961-3971.
- 30 Soletti L, Hong Y, Guan J, Stankus J, El-Kurdi M, Wagner W, Vorp D: A bilayered elastomeric scaffold for tissue engineering of small diameter vascular grafts. *Acta Biomater* 2010;6:110-122.
- 31 Shimizu K, Ito A, Arinobe M, Murase Y, Iwata Y, Narita Y, Kagami H, Ueda M, Honda H: Effective cell-seeding technique using magnetite nanoparticles and magnetic force onto decellularized blood vessels for vascular tissue engineering. *J Biosci Bioeng* 2007;103:472-478.
- 32 Doshi K: Direct cell seeding on collagen-coated silicone mandrels to generate cell-derived tissue tubes: Biomedical Engineering. Worcester, Worcester Polytechnic Institute, 2009, Master of Science, pp 85.
- 33 Grenier G, Remy-Zolghadri M, Guignard R, Bergeron F, Labbe R, Auger F, Germain L: Isolation and culture of the three vascular cell types from a small vein biopsy sample. *In Vitro Cell Dev Biol Anim* 2003;39:131-139.
- 34 Zhang W, Liu W, Cui L, Cao Y: Tissue engineering of blood vessel. *J Cell Mol Med* 2007;11:945-957.
- 35 Niklason L, Langer R: Advances in tissue engineering of blood vessels and other tissues. *Transpl Immunol* 1997;5:303-306.

- 36 Kestendjieva S, Kyurkchiev D, Tsvetkova G, Mehandjiev T, Dimitrov A, Nikolov A, Kyurkchiev S: Characterization of mesenchymal stem cells isolated from the human umbilical cord. *Cell Biol Int* 2008;32:724-732.
- 37 Lakshmipathy U, Verfaillie C: Stem cell plasticity. *Blood Rev* 2005;19:29-38.
- 38 Baksh D, Yao R, Tuan R: Comparison of proliferative and multilineage differentiation potential of human mesenchymal stem cells derived from umbilical cord and bone marrow. *Stem Cells* 2007;25:1384-1392.
- 39 Deans R, Moseley A: Mesenchymal stem cells: Biology and potential clinical uses. *Exp Hematol* 2000;28:875-884.
- 40 Jiang Y, Jahagirdar B, Reinhardt R, Schwartz R, Keene C, Ortiz-Gonzalez X, Reyes M, Lenvik T, Lund T, Blackstad M, Du J, Aldrich S, Lisberg A, Low W, Largaespada D, Verfaillie C: Pluripotency of mesenchymal stem cells derived from adult marrow. *Nature* 2002;418:41-49.
- 41 Baxter M, Wynn R, Jowitt S, Wraith J, Fairbairn L, Bellantuono I: Study of telomere length reveals rapid aging of human marrow stromal cells following in vitro expansion. *Stem Cells* 2004;22:675-682.
- 42 Kemp K, Hows J, Donaldson C: Bone marrow-derived mesenchymal stem cells. *Leuk Lymphoma* 2005;46:1531-1544.
- 43 Peng L, Li H, Gu L, Peng X, Huang Y, Gao Z: Comparison of biological characteristics of marrow mesenchymal stem cells in hepatitis b patients and normal adults. *World J Gastroenterol* 2007;13:1743-1746.
- 44 Hashi C, Zhu Y, Yang G, Young W, Hsiao B, Wang K, Chu B, Li S: Antithrombogenic property of bone marrow mesenchymal stem cells in nanofibrous vascular grafts. *Proc Natl Acad Sci U S A* 2007;104:11915-11920.
- 45 Gong Z, Niklason L: Small-diameter human vessel wall engineered from bone marrow-derived mesenchymal stem cells (hmscs). *FASEB J* 2008;22:1635-1648.
- 46 Galmiche M, Koteliansky V, Brière J, Hervé P, Charbord P: Stromal cells from human long-term marrow cultures are mesenchymal cells that differentiate following a vascular smooth muscle differentiation pathway. *Blood* 1993;82:66-76.
- 47 Jockenhoevel S, Zund G, Hoerstrup S, Chalabi K, Sachweh J, Demircan L, Messmer B, Turina M: Fibrin gel -- advantages of a new scaffold in cardiovascular tissue engineering. *Eur J Cardiothorac Surg* 2001;19:424-430.

- 48 Mol A, van Lieshout M, Dam-de Veen C, Neuenschwander S, Hoerstrup S, Baaijens F, Bouten C: Fibrin as a cell carrier in cardiovascular tissue engineering applications. *Biomaterials* 2005;26:3113-3121.
- 49 Bensaïd W, Triffitt J, Blanchat C, Oudina K, Sedel L, Petite H: A biodegradable fibrin scaffold for mesenchymal stem cell transplantation. *Biomaterials* 2003;24:2497-2502.
- 50 Swartz D, Russell J, Andreadis S: Engineering of fibrin-based functional and implantable small-diameter blood vessels. *Am J Physiol Heart Circ Physiol* 2005;288:H1451-1460.
- 51 Catelas I, Sese N, Wu B, Dunn J, Helgerson S, Tawil B: Human mesenchymal stem cell proliferation and osteogenic differentiation in fibrin gels in vitro. *Tissue Eng* 2006;12:2385-2396.
- 52 O'Cearbhaill E, Murphy M, Barry F, McHugh P, Barron V: Behavior of human mesenchymal stem cells in fibrin-based vascular tissue engineering constructs. *Ann Biomed Eng* 2010
- 53 Cornwell K, Pins G: Discrete crosslinked fibrin microthread scaffolds for tissue regeneration. *J Biomed Mater Res A* 2007;82:104-112.
- 54 Jones L, Gray M, Yue S, Haugland R, Singer V: Sensitive determination of cell number using the cyquant cell proliferation assay. *J Immunol Methods* 2001;254:85-98.
- 55 Cornwell K, Lei P, Andreadis S, Pins G: Crosslinking of discrete self-assembled collagen threads: Effects on mechanical strength and cell-matrix interactions. *J Biomed Mater Res A* 2007;80:362-371.
- 56 Soletti L, Nieponice A, Guan J, Stankus J, Wagner W, Vorp D: A seeding device for tissue engineered tubular structures. *Biomaterials* 2006;27:4863-4870.
- 57 Barry F, Boynton R, Liu B, Murphy J: Chondrogenic differentiation of mesenchymal stem cells from bone marrow: Differentiation-dependent gene expression of matrix components. *Exp Cell Res* 2001;268:189-200.
- 58 Bruder S, Ricalton N, Boynton R, Connolly T, Jaiswal N, Zaia J, Barry F: Mesenchymal stem cell surface antigen sb-10 corresponds to activated leukocyte cell adhesion molecule and is involved in osteogenic differentiation. *J Bone Miner Res* 1998;13:655-663.
- 59 Muraglia A, Cancedda R, Quarto R: Clonal mesenchymal progenitors from human bone marrow differentiate in vitro according to a hierarchical model. *J Cell Sci* 2000;113 ( Pt 7):1161-1166.



- 60 Gérard C, Blouin K, Tchernof A, Doillon C: Adipogenesis in nonadherent and adherent bone marrow stem cells grown in fibrin gel and in the presence of adult plasma. *Cells Tissues Organs* 2008;187:186-198.
- 61 Megan M: Fibrin microthreads promote stem cell growth for localized delivery in regenerative therapy, 2008,
- 62 Kassem M, Abdallah B: Human bone-marrow-derived mesenchymal stem cells: Biological characteristics and potential role in therapy of degenerative diseases. *Cell Tissue Res* 2008;331:157-163.
- 63 Xu W, Zhang X, Qian H, Zhu W, Sun X, Hu J, Zhou H, Chen Y: Mesenchymal stem cells from adult human bone marrow differentiate into a cardiomyocyte phenotype in vitro. *Exp Biol Med (Maywood)* 2004;229:623-631.